

AHMET ERKAN KILIÇ

**REDESIGN OF DRIVETRAIN COMPONENT OF A SHELL ECO
MARATHON VEHICLE FOR ADDITIVE MANUFACTURING VIA
TOPOLOGY OPTIMIZATION**

M. Sc. THESIS

AHMET ERKAN KILIÇ

2020

İRİ REİS UNIVERSITY

2020

REDESIGN OF DRIVETRAIN COMPONENT OF A SHELL ECO MARATHON
VEHICLE FOR ADDITIVE MANUFACTURING VIA
TOPOLOGY OPTIMIZATION

by

Ahmet Erkan KILIC

B. S., Metallurgical & Materials Engineering, Sakarya University, 2003

M. S., Business Administration, Yeditepe University, 2010

Submitted to the Institute for Graduate Studies in
Science and Engineering in partial fulfillment of
the requirements for the degree of
Master of Science

Graduate Program in Mechanical Engineering
Pîrî Reis University
2020

**REDESIGN OF DRIVETRAIN COMPONENT OF A SHELL ECO
MARATHON VEHICLE FOR ADDITIVE MANUFACTURING VIA
TOPOLOGY OPTIMIZATION**

APPROVED BY:

Dr. Lect. H. Yavuz Yucesoy
(Thesis Supervisor)

Dr. Lect. Atilla Savas
(Thesis Co-Supervisor)

Assoc. Prof. Dr. Ertan Öcalan
(Committee Member)

Assoc. Prof. Dr. Serkan Nohut
(Committee Member)

Prof. Dr. M. Oktay Almak
(Committee Member)

DATE OF APPROVAL:

DEDICATION



Dedicated to my family:
My wife Asli,
My daughter Kayra,
My parents Ayse and Mithat,
And my brother Mustafa.

ACKNOWLEDGEMENTS

This thesis constitutes the final portion of my masters study in Mechanical Engineering at Piri Reis University. I would like to take this opportunity to express my sincere appreciation to a few people.

First of all, I would like to thank my Supervisor Dr. Lect. H. Yavuz Yucesoy for allowing me to work on this thesis under his invaluable direction. I also would like to thank my Co-Supervisor Dr. Lect. Atilla Savas for his strong support during this cycle.

I am grateful to SAITEM Team from Sakarya University who accepted to work with me on this topic. I wish to express special thanks to Eray Agalar, mechanical design lead from SAITEM Team. I appreciate his help, cooperation and willingness to exchange information during this thesis.

Finally, I would like to thank to my family, especially to my wife Asli and my daughter Kayra for their support and patience during this period.

ABSTRACT

REDESIGN OF DRIVETRAIN COMPONENT OF A SHELL ECO MARATHON VEHICLE FOR ADDITIVE MANUFACTURING VIA TOPOLOGY OPTIMIZATION

Additive Manufacturing (AM) has been an emerging technology and an important alternative to conventional manufacturing methods as it enables production of lighter parts that are potentially more durable.

In this context, the design for additive manufacturing (DFAM) has been drawing considerable amount of attention mainly in aerospace, automotive industries as well as in academia.

On the other hand, the ability of additive manufacturing to manufacture complex topology often is the outcome from topology optimization, makes topology optimization a good design tool for additive manufacturing.

The use of lighter and more durable components is of critical importance in aerospace and automotive industries due to the goals for more efficient use of the energy resources and / or higher performance.

The main objective of the present work is to redesign a structural component of the drivetrain of the Shell Eco-Marathon vehicle, SAITEM EVRIM-4, with the use of Altair Inspire™, an industrial generative design tool, by application of Topology Optimization for Additive Manufacturing aiming mass reduction.

The results of finite element analysis that have been performed as part of the present work clearly show that the redesigned part is capable of withstanding to applied loads while the part is in operation.

Moreover, a significant mass reduction is achieved with the redesigned model.

ÖZET

SHELL ECO MARATHON ARACININ AKTARMA ORGANI BİLEŞENİNİN KATMANLI İMALAT ÜRETİMİ İÇİN TOPOLOJİ OPTİMİZASYONU İLE YENİDEN TASARLANMASI

Katmanlı İmalat, potansiyel olarak daha mukavim ve daha hafif parçaların üretilmesini mümkün kıldığından, geleneksel üretim yöntemlerine önemli bir alternatif olarak ortaya çıkan bir teknolojidir.

Katmanlı İmalat ile üretimi gerçekleştirilen hafif yapıların tasarımı, özellikle havacılık, otomotiv endüstrisi ve akademide büyük dikkat çekmektedir.

Öte yandan, katmanlı imalatın karmaşık topoloji üretme kabiliyeti, genellikle topoloji optimizasyonunun getirdiği bir sonuçtur ki, bu da topoloji optimizasyonunu katmanlı imalat için iyi bir tasarım aracı kılmaktadır.

Enerji kaynaklarının daha verimli kullanılması ve / veya daha yüksek performans sağlama hedefleri nedeniyle, daha hafif ve daha dayanıklı bileşenlerin kullanılması havacılık ve otomotiv endüstrilerinde kritik öneme sahiptir.

Bu çalışmanın temel amacı, Shell Eco-Marathon aracı SAITEM EVRIM-4'ün aktarma organındaki yapısal bir bileşenin, Topoloji Optimizasyonu uygulaması ile, endüstriyel bir tasarım aracı olan Altair Inspire™ kullanılarak, kütle azaltma amacıyla yeniden tasarlanmasıdır.

Mevcut çalışmanın bir parçası olarak gerçekleştirilen sonlu elemanlar analizi sonuçları, yeniden tasarlanmış parçanın, parça çalışırken maruz kalacağı yüklere dayanabileceğini açıkça göstermektedir.

Ayrıca, yeniden tasarlanmış model ile önemli ölçüde bir ağırlık azaltma elde edilmiştir.

TABLE OF CONTENTS

DEDICATION	iii
ACKNOWLEDGEMENTS	iv
ABSTRACT	v
ÖZET	vi
TABLE OF CONTENTS	vii
TABLE OF FIGURES	ix
LIST OF SYMBOLS / ABBREVIATIONS	xi
1. INTRODUCTION	1
1.1. Background	1
1.2. Scope	2
1.3. Structure of the Thesis Report.....	3
2. ADDITIVE MANUFACTURING.....	5
2.1. What is Additive Manufacturing?.....	5
2.2. Additive Manufacturing Categories.....	5
2.3. Additive Manufacturing Process Steps	7
2.4. Material Options for Additive Manufacturing	8
3. TOPOLOGY OPTIMIZATION.....	9
3.1. Optimization.....	9
3.2. What is Topology Optimization?.....	9
3.3. AM and Topology Optimization – A Perfect Couple	12
3.4. Review of Commercial Software Packages for TO	12
4. DRIVE TRAIN OF EVRIM-4 VEHICLE	14
4.1. Drive Train of Evrim-4 Vehicle.....	14
4.2. Electric Motor Bracket.....	16

4.3.	Power and Torque Calculation.....	18
4.4.	Gear Force Analysis.....	22
5.	DESIGN FOR ADDITIVE MANUFACTURING	26
5.1.	Definition of Design and Non-Design Spaces	27
5.2.	Definition of Loads, Constraints and Material Properties	28
5.3.	Applying Shape Controls	29
5.4.	Topology Optimization Run	31
5.5.	Interpretation of Topology Optimization Results	33
5.6.	Setting Design Criteria.....	34
5.7.	Part Redesign with Inspire PolyNURBS.....	35
5.8.	Rendering with Evolve.....	36
6.	RESULTS AND DISCUSSION.....	39
6.1.	Mass of the Redesigned Model.....	39
6.2.	Waste Minimization with the Redesigned Model.....	39
6.3.	Finite Element Analysis of PolyNURBS Results	40
6.4.	Interpretation of Finite Element Analysis Results	44
7.	CONCLUSIONS AND RECOMMENDATIONS.....	46
	REFERENCES.....	47
	CURRICULUM VITAE	50

TABLE OF FIGURES

Figure 1-1 Photography of the EVRIM-4	3
Figure 2-1 The process scheme for additive manufacturing	7
Figure 2-2 Commonly used materials in additive manufacturing	8
Figure 3-1 Different types of optimization.....	9
Figure 3-2 Example of Topology Optimization Problem.	11
Figure 4-1 A generic view of the drive train system of Evrim-4.	14
Figure 4-2 Components of the drive train system of Evrim-4.	15
Figure 4-3 Bracket Assembly View.....	16
Figure 4-4 Bracket Assembly View	15
Figure 4-5 Original design of electric motor bracket.....	16
Figure 4-6 Maxon RE 50 D.C. motor (PN 370354).....	17
Figure 4-7 Maxon RE 50 D.C. motor (PN 370354) Technical Data.....	18
Figure 4-8 D.C. Motor Torque-Speed Curve	18
Figure 4-9 D.C. Motor Speed – Torque Curve Showing Ranges.....	19
Figure 4-10 D.C. Motor Torque Speed Curve.....	20
Figure 4-11 Torque - Speed Curve of Maxon RE 50 D.C. Motor	21
Figure 4-12 D.C. Motors and Gear Train.....	22
Figure 4-13 FBD of Acting Forces at the Pitch Point C of the Pinion.....	24
Figure 4-14 Pinion 1 and Driven Gear.....	25
Figure 4-15 Pinion 2 and Driven Gear	25
Figure 5-1 Process Map of Design Steps	26
Figure 5-2 Design and Non-Design Spaces.	27
Figure 5-3 Design and Non-Design Spaces.	28
Figure 5-4 Material data[26] [27] for AlSi10Mg	29
Figure 5-5 Applied Loads and Constraints.....	30
Figure 5-6 A Different View of Applied Loads and Constraints	30
Figure 5-7 Part After Topology Optimization Run.....	32
Figure 5-8 Another View of the Part After Topology Optimization Run	32
Figure 5-9 von Misses Stress Analysis Results of the Optimized Model	33
Figure 5-10 Redesigned Model with the Use of PolyNURBS.....	35

Figure 5-11 Another View of Redesigned Model with the use of PolyNURBS.....	36
Figure 5-12 Image of Redesigned Model After Rendering in Evolve Software.....	37
Figure 5-13 Another Image of Redesigned Model After Rendering in Evolve	37
Figure 5-14 Another Image of Redesigned Model After Rendering in Evolve	38
Figure 6-1 Analysis Results for Factor of Safety for Yielding.	40
Figure 6-2 Analysis of FoS for Yielding Showing Minimum FoS Location.....	41
Figure 6-3 Analysis of FoS for Yielding Showing Minimum FoS Location.....	41
Figure 6-4 Analysis Results for Ultimate Factor of Safety	42
Figure 6-5 Analysis of Ultimate FoS Showing Minimum Ultimate FoS Location....	42
Figure 6-6 Analysis of Ultimate FoS Showing Minimum Ultimate FoS Location....	43
Figure 6-7 Analysis Results for von Misses Stress	43
Figure 6-8 von Misses Stress Analysis Showing Maximum Stress Location.....	44

LIST OF SYMBOLS / ABBREVIATIONS

3D : Three Dimensional
7075 Al : 7075 Aluminum
ABS : Acrylonitrile butadiene styrene
AM : Additive Manufacturing
AMF : Additive Manufacturing File Format
ASTM : American Society for Testing and Materials
ATOM : Abaqus™ Topology Optimization Module
CAD : Computer-Aided Design
CAE : Computer-Aided Engineering
CTE : Coefficient of Thermal Expansion
 d_l = Pitch Diameter of Pinion
D.C. : Direct Current
DED : Directed Energy Deposition
DFAM : Design for Additive Manufacturing
E: Modulus of Elasticity
FEA : Finite Element Analysis
FFF : Freeform Fabrication
FoS : Factor of Safety
ISO : International Organization for Standardization
m : Module
MIT : Massachusetts Institute of Technology
 m_n = Normal Module
NVH : Noise, Vibration and Harshness
PEEK : Polyether ether ketone
 P_{max} : Maximum Power
RP : Rapid Prototyping
RPM : Revolutions per Minute
SAITEM : Sakarya University Advanced Technologies Group
SIMP : Solid Isotropic Material with Penalization
STL : Stereolithography

T : Torque

TO : Topology Optimization

TPE : Thermoplastic elastomer

T_s : Stall Torque

UV : Ultraviolet

V : Pitch Line Velocity

W_n : No Load Speed

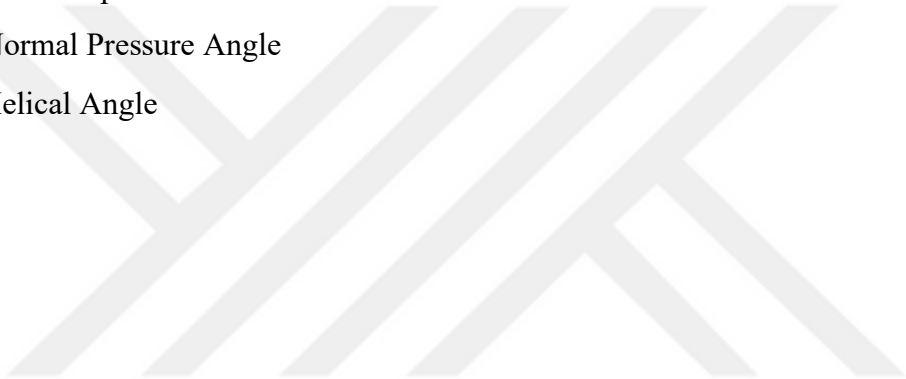
Z : Number of Teeth on a Gear

ω : Rotational Speed

ω_n : No-load Speed

Φ_n = Normal Pressure Angle

Ψ = Helical Angle



1. INTRODUCTION

1.1. Background

American Society for Testing and Materials defines Additive Manufacturing as a materials joining process in which parts and/or components are manufactured in multiple layers from the *3D CAD* model. [1]

The abbreviation that is typically used for Additive Manufacturing is *AM*. With additive manufacturing technology, it is much simpler to produce parts with complicated geometry directly from their *3D* models. [2]

Some of the main advantages and capabilities of the *3D* metal printing technology are mass reduction, freedom of design, enabling production of complex structures and in-process scrap material reduction. [3]

As Additive Manufacturing offers freedom of design, one of the most important benefits of *AM* over conventional manufacturing methods is its capability to produce very complicated shapes or geometries. [4]

Topology optimization is a numerical method which aims to find out the optimum material lay-out or the part geometry within the existing design space taking the restrictions, such as the boundary conditions and constraints, and applied loads into account. The outcome is typically a more lightweight part that can still meet the design intend and criteria. [5]

For this reason, the combination of additive manufacturing and topology optimization capabilities can be an excellent match. [4]

Shell Eco Marathon is a world-wide competition for student teams to which they participate with their vehicles. The aim of the competition is to encourage students to design and manufacture their vehicles through high-tech and energy-efficient solutions. [6]

In the competition, vehicles are classified by design and by energy resource. The two vehicle design classes in the competition are [6]:

- i) UrbanConcept: In this design class, vehicles are similar to modern automobiles.
- ii) Prototype: Vehicle design class where ultra-efficiency is the most important parameter. Three wheel vehicle design is more common in this class.

In addition to design classes, below are the vehicle classes by energy source [6]:

- i) Internal Combustion Vehicles
- ii) Electric Vehicles
- iii) Hydrogen Vehicles

SAITEM (Sakarya University Advanced Technologies Group) has been competing in Shell Eco-Marathon for some time in different categories and the team has achieved significant national and international success with their electric propulsion (EVRIM) and hydrogen fueled cars (SAHIMO).

With SAHIMO, the team achieved the 1st rank on the national scale and 3rd rank on the international scale in Europe in 2008 and 2009. And with EVRIM, the team achieved the 1st rank in 2012, 2013 and 2014 on the national scale; and 7th rank in 2012 and 2013 and 8th rank in 2014 on the international scale in Europe.

SAITEM has been participating the Shell Eco-Marathon in “Urban Concept” Electric propulsion category with EVRIM-4 vehicle.

The objective of Shell Eco-Marathon is to build the most energy-efficient car. Therefore, the weight of the car components is of critical importance.

1.2. Scope

The aim of this master thesis is to redesign the Electric Motor Bracket, a structural component in the drive train of EVRIM-4 Shell Eco-Marathon vehicle, using the generative design and topology optimization software Altair Inspire™ for mass reduction.

Along with the engineering calculations required for the redesign operation, results of the redesign work, an overview of additive manufacturing technology, topology

optimization, the drivetrain of EVRIM-4 vehicle and the design for additive manufacturing method that was followed in Altair Inspire™ will be provided.

The scope of this master thesis is limited to redesigning of the EVRIM-4 drivetrain component and does not cover the print process.



Figure 1-1 Photography of the EVRIM-4

1.3. Structure of the Thesis Report

The present master thesis is structured as follows:

First, the background information will be provided relating to Additive Manufacturing in Chapter 2. Then, Topology Optimization will be explained in Chapter 3. Following those, In Chapter 4, an overview of the drive train of Shell Eco-Marathon vehicle EVRIM-4, the original design of the Electric Motor Bracket that is aimed to be redesigned within the scope of this thesis, and engineering calculations relating to loads that apply on the Electric Motor Bracket that are necessary to perform optimization of the original design will be provided. Following that, process steps relating to redesign of the Electric Motor Bracket and all relevant Finite Element Analysis results will be given in Chapter 5. Results are discussed in

Chapter 6. The final chapter, Chapter 7, concludes the work and places recommendations for future work.



2. ADDITIVE MANUFACTURING

2.1. What is Additive Manufacturing?

Additive Manufacturing has been a very attractive and innovative technology lately. And, it is expected that *AM* will be one of the most influential technologies in the next few decades. [7] Various terms such as Rapid Prototyping, Freeform Fabrication, 3D Printing are also used to refer to Additive Manufacturing. [8]

The first additive manufacturing method, namely Stereolithography, was developed by Charles Hull, the co-founder of 3D Systems, in 1980's. SLA-1 was the first additive manufacturing machine that was marketed by the same company. [9] Thanks to advances in technology, *AM* can now be used not only for prototyping, but also for manufacturing of final products. [2]

One of the distinctive nature of *AM* process is to form the part in multiple layers, in other words, layer-upon-layer. The *CAD* model of the part is processed and the part is built in thin cross-sectional layers. Comparing to conventional manufacturing techniques, this technique makes production of very complicated geometries more producible and at a lower manufacturing cost. [10] Additive manufacturing technique is the converse of conventional subtractive manufacturing techniques as the part is constructed in layers added on another; however in subtractive techniques, rather than adding material, unnecessary material is typically removed (e.g. as in the case of turning, hole making, milling processes) to get the finished part. [5]

2.2. Additive Manufacturing Categories

As per *ASTM 2792-12* [1], American Society of Testing Materials classifies additive manufacturing technologies into 7 categories as listed below:

- 1) Powder Bed Fusion
- 2) Directed Energy Deposition
- 3) Material Jetting
- 4) Binder Jetting
- 5) Vat Photopolymerization
- 6) Sheet Lamination
- 7) Material Extrusion

According to [2], brief descriptions of those additive manufacturing technologies are as follows:

In powder bed fusion process, a metal, polymer or ceramic powder filled in a chamber is selectively fused in thin layers with an energy source such as laser or electron beam.

In *DED* (Directed Energy Deposition) method, the feedstock material, either in the form of powder or wire, is fed into a nozzle with manipulation capability; and is melted with the use of an energy source and at the same time deposited layer by layer to form the geometry. Although ceramic and polymer feedstock materials can be deposited with the *DED* method, it is mostly applied to deposit metal powders.

In material jetting process, typically a photopolymer is jetted in *3D* with the use of printheads and exposed to *UV* light for polymerization.

In binder jetting process, the binder material is selectively jetted into the primary material in the powder bed via printheads to build the geometry. The process was invented at *MIT* in 1990s with the name of *3D* Printing (*3DP*). The binder jetting method has many common advantages of both material jetting and powder bed fusion processes when compared to other *AM* techniques.

In vat photopolymerization technique, a liquid curable resin that is filled in a vat is selectively cured with the use of radiation such as *UV* light to build the part geometry layer upon layer. Stereolithography is considered as one of the vat photopolymerization processes.

In sheet lamination technique, the final part is obtained through cutting and bonding of material (typically polymer, paper or metal sheet laminates) layer by layer.

In the material extrusion process, the feedstock material is melted with heat in a chamber and then extruded through a nozzle that is manipulated to deposit material in the semi-molten state.

2.3. Additive Manufacturing Process Steps

The process flow for additive manufacturing is defined in eight main steps according to [2]. This process flow map is given in Figure 2.1.

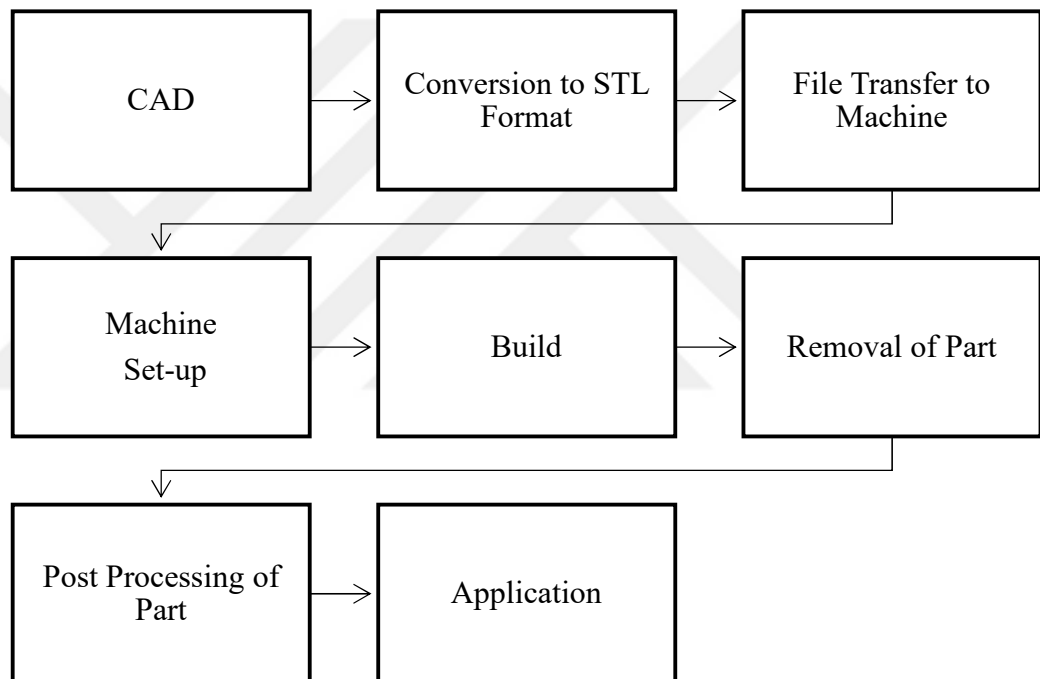


Figure 2-1 The process flow map for additive manufacturing

In the first step of the additive manufacturing process flow, the part design is generated with a *CAD* software. Then, the generated *3D CAD* file is converted to *STL* (Stereolithography Tessellation Language) format as almost all additive manufacturing equipment utilizes this format. Once this is complete, the *STL* file is transferred to the additive manufacturing equipment. Following this, printing process parameters are set-up and the printing process is started. Upon completion of the printing process, the part is removed from the equipment. This is followed by the post-processing such as cleaning or removal of support structures in order to get the finished part that is ready for use. [2]

The *STL* file format is very common for majority of the additive manufacturing machines; however, newer file formats such as *AMF* (Additive Manufacturing File Format) and *3MF* (3D Manufacturing Format), with improved features comparing to *STL* file format, have started to become available. [11]

2.4. Material Options for Additive Manufacturing

A broad range of materials are available for use as a feedstock material in additive manufacturing. Some examples of those materials are presented in Figure 2.2.[5]

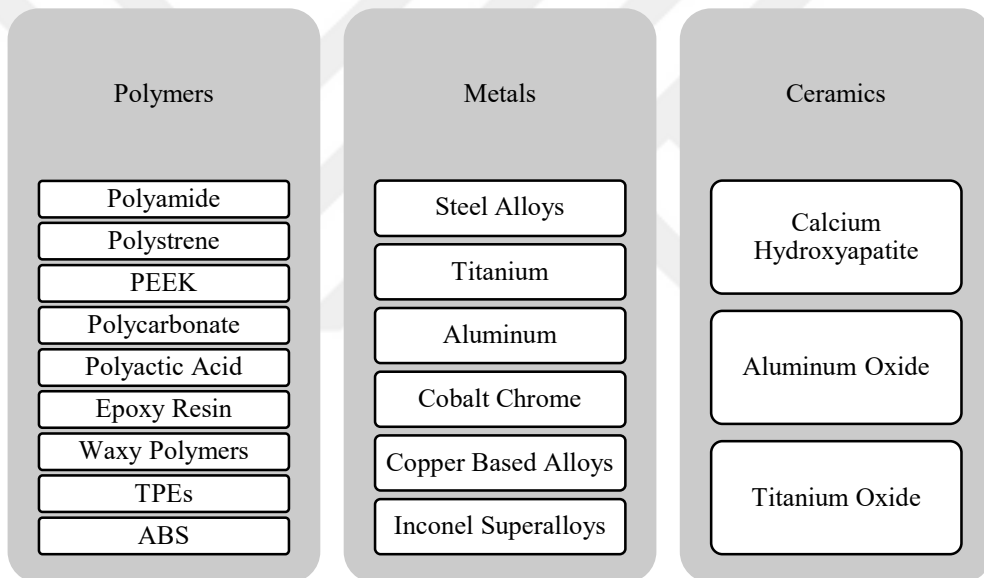


Figure 2-2 Examples of materials that are commonly used in additive manufacturing

3. TOPOLOGY OPTIMIZATION

3.1. Optimization

Depending on the goal of the optimization problem, three types of optimization in design can be utilized. Those three optimization approaches and their brief definitions are given below: [2],

- *Size optimization* – dimensional values of a geometry are determined in size optimization
- *Shape optimization* – the spatial form or contours of part surfaces are modified in shape optimization
- *Topology optimization* – material distributions are examined to find the optimum lay-out in topology optimization

Graphical representations of those three optimization types are given in Figure 3.1. below. [12]

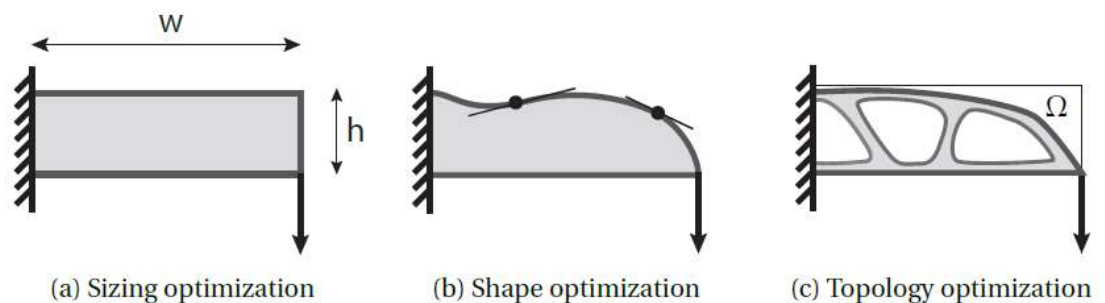


Figure 3-1 Three different types of optimization

3.2. What is Topology Optimization?

As also highlighted in Introduction chapter, topology optimization (*TO*) can be defined as an optimization method that is based on a numerical background with the objective of

finding out optimum material distribution within a given design space for the pre-determined restrictions, such as loads and boundary conditions. [5]

Unlike size and / or shape optimization, as being a free-form material lay-out method, topology optimization makes it possible to form, combine and divide the internal elements (e.g. voids, solids) of a part. For this reason, topology optimization may offer greater structural performance comparing to size optimization or shape optimization. [13]

Out of the available design technology tools, especially topology optimization (*TO*) is the most accepted in order to get the maximum benefit from the freedom of design property of additive manufacturing technology. [14]

Topology optimization (*TO*) techniques determine the arrangement of shape elements. The outputs of topology optimization are generally used as inputs to following size optimization or shape optimization problems. The calculation time in a topology optimization problem may require much time as structural finite element analyses are conducted throughout the duration of each iteration until the final optimization result. Typically, a topology optimization model is stressed almost completely across its geometry depending on the pre-defined loading conditions. [2]

Topology optimization can be applied on two distinct type of structures; continuum structures and discrete structures. In general, discrete structures relate to truss structures such as bridges. On the other hand, continuum structures relate to components that are smaller than truss structures.[15] Topology optimization methods can be classified into two such as truss based and volume based methods. Truss based *TO* methods are applied to discrete structures and density based *TO* methods are applied to continuum structures. [2]

The density-based topology optimization method is also known as *SIMP* (Solid Isotropic Material with Penalization) method. *SIMP* is the most accepted topology optimization method globally. Majority of topology optimization software programs are typically developed on the basis of the *SIMP* method. [2]

The initial geometry of the part is considered to be composed of volume elements in the *SIMP* method. The density of every single volume element takes values in an optimization problem. A value of 1 (one) refers to fully solid material and a value of 0 (zero) refer to voids, in other words no solid material. Any density values between 0 and 1 refer to

porous material. The final solution of optimization problem is developed based on the fully solid (density value of 1) or voids (density value of 0) by penalizing the stiffness of intermediate values in the *FEA* performed as part of the *SIMP TO* run. [2]

An example of a starting design and an optimized design are represented in Figure 3.2 [5]. In the optimization cycle, the material is distributed within the design space iteratively for the best or optimum result. The structural performance is reviewed by the use of *FEA* in each iteration.[5]

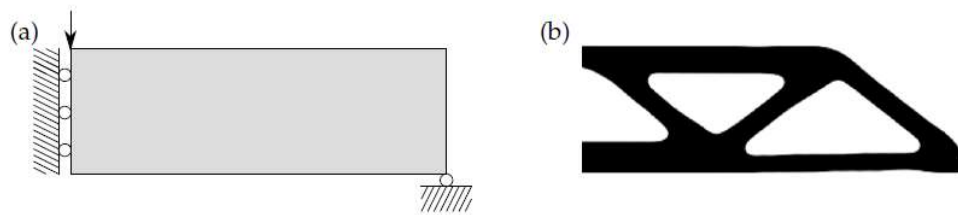


Figure 3-2 Example of Topology Optimization Problem.

(a) Design domain, including loads and supports. (b) Optimized design

According to [5], a *SIMP* method based topology optimization problem can be formulated as:

$$\begin{aligned}
 \min_{\mu} \quad & c(\mu) = U^T K U && \text{Compliance} && (3.1) \\
 \text{subject to} \quad & K U = F, && \text{Equilibrium state equation} \\
 & g(\mu) = V(\mu)/V^* - 1 \leq 0, && \text{Volume Constraint} \\
 & 0 \leq \mu_e \leq 1, \forall e \in \Omega && \text{Box constraints on design variables} \\
 & \dots && \text{Additional constraints}
 \end{aligned}$$

In the above formulation, μ represents the vector of design variables, c represents the compliance, U represents the global displacement vector, F represents global force vector, K represents the global stiffness matrix, g represents the volume constraint, V is the volume

of the material, V^* represent the maximum volume that can be allowed and e represents the index variable. [5]

3.3. AM and Topology Optimization – A Perfect Couple

Additive manufacturing provides a much more freedom of design in comparison to subtractive manufacturing methods such as machining. Its manufacturing cost structure is fully dissimilar to cost structure of subtractive manufacturing. With additive manufacturing technology, the complexity of part geometry is not the major contributor for the production cost any more. [14]

The technological progress in metal powder based additive manufacturing in the last 10 years has led to use of additive manufacturing for final products rather than its limited use for prototyping only. In order to take the full advantage of additive manufacturing, it is always a better approach to re-design the component rather than manufacturing it by utilizing its original design. [14], [16]

In this context, additive manufacturing and topology optimization are a perfect couple. Additive manufacturing enables producing very complex geometries where topology optimization offers taking the advantage of freedom of design provided by additive manufacturing. [5]

3.4. Review of Commercial Software Packages for TO

Driven by the increased need and use for *TO* applications in Design for *AM*, there has been a significant progress also in *TO* software products in terms of the number of software packages, their providers and the maturity of the products. [17]

In this present work, only a few of the most popular software products will be discussed, that are namely Abaqus™, Altair OptiStruct™ and Altair Inspire™.

Abaqus™ is a software product of Dassault Systemes and covered under the Simulia brand. It is an *FEA* software that offers capability to perform nonlinear and plasticity analyses. Abaqus™ also has a very wide range of material models in its material library.[2]

With Abaqus Topology Optimization Module, topology and shape optimization can be performed. [2]

Another topology optimization software package to be reviewed is OptiStruct™ which is an industry leading product of Altair. It offers linear and nonlinear structural analysis for both static and dynamic loading conditions. [2]

Inspire™ is another topology optimization software from Altair which offers easy-to-use generative design and topology optimization capabilities. [18]

In this current study, free student edition of Altair Inspire™ 2019.1 was used as the tool of choice for the redesign of EVRIM-4's Electric Motor Bracket.

Altair Inspire™ is based on Altair OptiStruct™ technology in the background and it allows designers to generate new concepts via its easy-to-use interface to achieve optimized structures in shorter engineering turnaround time. [19]

Altair Inspire™ offers to perform topology optimization and finite element analysis. Material properties can be assigned either from its customizable material library. Additionally, Inspire™ has a PolyNURBS feature with which free-form solid geometries can be created to produce finished product via *AM*. [20]

4. DRIVE TRAIN OF EVRIM-4 VEHICLE

In this section, an overview of the drive train of Evrim-4 vehicle will be given. In addition, engineering calculations to define the loads and constraints to which the Electric Motor Bracket is subject to will be provided, as topology optimization is a finite element analysis (*FEA*) based approach that generates an optimal material layout of a structure within a given design space.

4.1. Drive Train of Evrim-4 Vehicle

Figure 4.1 represents a generic photo of the drive train system and Figure 4.2 shows the components of the drivetrain system more in detail.

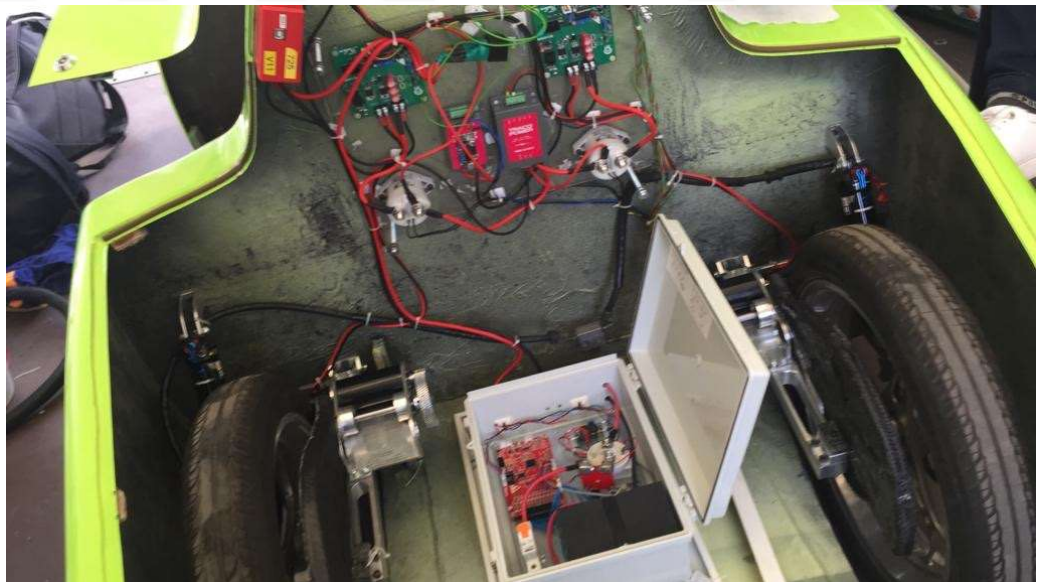


Figure 4-1 A generic view of the drive train system of Evrim-4.

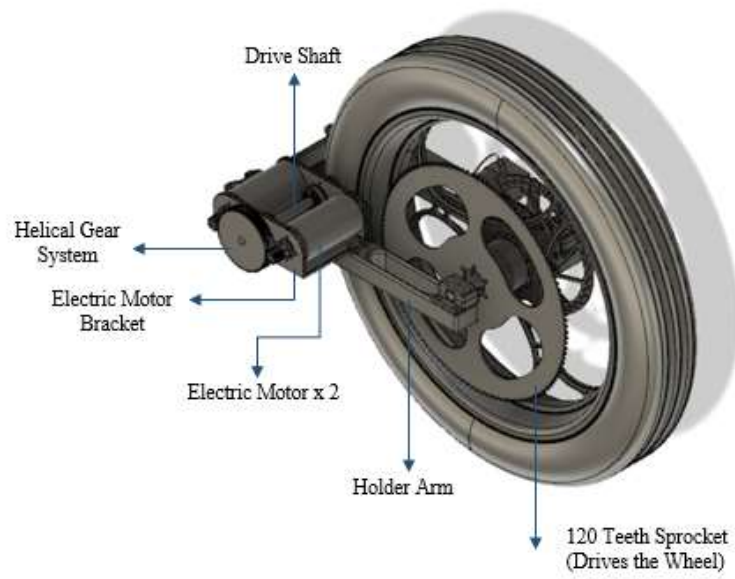


Figure 4-2 Components of the drive train system of Evrim-4.

Figure 4.3 and Figure 4.4 represent a more detailed view of the *D.C.* motor, gearbox, transmission shaft and electric motor bracket assembly.

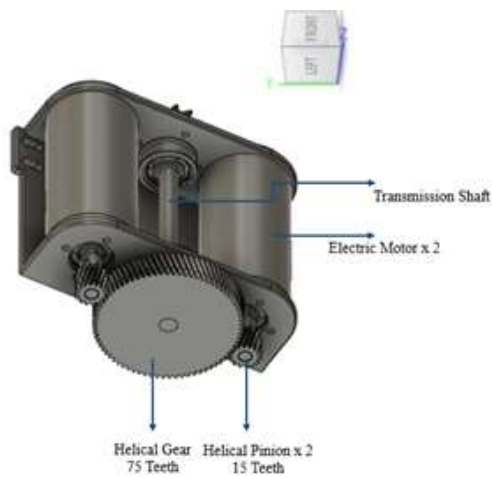


Figure 4-3 Bracket Assembly View

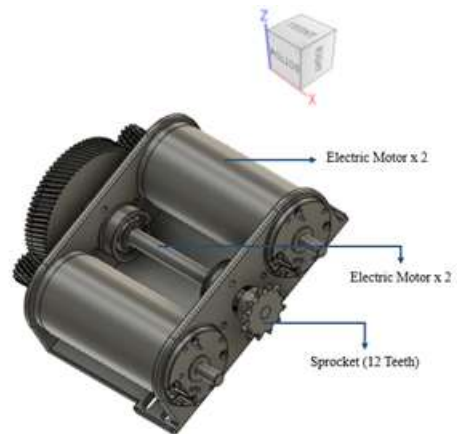


Figure 4-4 Bracket Assembly View

The principal working mechanism of the drivetrain system is as follows:

15 teeth helical pinions (see Figure 4.3) with 20° normal pressure angle, 1 mm normal module and a helix angle of 20° are keyed to the 2 x *D.C.* motor (2 x Maxon RE 50) shafts. Both of the 15 teeth helical pinions drive the 75 teeth helical gear (see Figure 4.3) in the middle which is keyed to transmission shaft. The transmission shaft drives the 12 teeth sprocket (see Figure 4.4) and the power is transmitted to other sprocket having 120 teeth (see Figure 4.2) through a transmission chain that is engaged with the sprockets. And the sprocket having 120 teeth drives the rear wheel.

As for the above defined drivetrain system, there are two of this drivetrain system in the vehicle that transmits power to both of the rear wheels of the vehicle.

4.2. Electric Motor Bracket

Electric motor bracket that is to be studied in this project is aimed to be redesigned for additive manufacturing using generative design methods in order to achieve mass reduction.

The main reason behind the selection of electric motor bracket is because it is the second heaviest structural component in the drivetrain; and additionally, its size and geometry make it quite feasible for additive manufacturing.

The original design of the electric motor bracket is shown in Figure 4.5. As can also be seen from Figure 4.3 and Figure 4.4, electric motor bracket to be studied in this thesis is designed to fit two electric motors on each one of the right and left rear side of the car.



Figure 4-5 Original design of electric motor bracket

The mass of the electric motor bracket is 364 grams; and there are two motor brackets in the car, making a total mass of 728 grams. The electric motor bracket is originally made of 7075 Al alloy.

In the original design, electric motor bracket is manufactured with subtractive techniques by machining a 7075 Al alloy billet. Per Altair Inspire results, it is calculated that 2837 grams of 7075 aluminum alloy billet would be needed to produce the electric motor bracket via the mentioned conventional subtractive techniques. Therefore, 87% of the material may be wasted in the conventional subtractive manufacturing methods while producing the electric motor bracket.

Evrin-4 is equipped with Maxon RE 50 electric motor. A photo of the electric motor is given in Figure 4.6.[21]



Figure 4-6 Maxon RE 50 D.C. motor (PN 370354)

Technical data and specifications of the Maxon RE 50 D.C. Motor (RE 50 \varnothing 50 mm, Graphite Brushes, 200 Watt) is given in Figure 4.7 [22] below:

Industrial Version IP54*		370354	389089
Motor Data			
Values at nominal voltage			
1	Nominal voltage	V	24
2	No load speed	rpm	5950
3	No load current	mA	236
4	Nominal speed	rpm	5680
5	Nominal torque (max. continuous torque)	mNm	405
6	Nominal current (max. continuous current)	A	10.8
7	Stall torque	mNm	8920
8	Stall current	A	232
9	Max. efficiency	%	94
Characteristics			
10	Terminal resistance	Ω	0.103
11	Terminal inductance	mH	0.072
12	Torque constant	mNm/A	38.5
13	Speed constant	rpm/V	248
14	Speed / torque gradient	rpm/mNm	0.668
15	Mechanical time constant	ms	3.75
16	Rotor inertia	gcm ²	536
Specifications			
Thermal data			
17	Thermal resistance housing-ambient	K/W	3.8
18	Thermal resistance winding-housing	K/W	1.2
19	Thermal time constant winding	s	71.7
20	Thermal time constant motor	s	1370
21	Ambient temperature	°C	-30...+100
22	Max. winding temperature	°C	+125
Mechanical data (preloaded ball bearings)			
23	Max. speed	rpm	9500
24	Axial play at axial load < 11.5 N	mm	0
	> 11.5 N	mm	0.1
25	Radial play	mm	preloaded
26	Max. axial load (dynamic)	N	30
27	Max. force for press fits (static) (static, shaft supported)	N	150
		N	6000
28	Max. radial load, 15 mm from flange	N	110
Other specifications			
29	Number of pole pairs		1
30	Number of commutator segments		15
31	Weight of motor	g	1100

Figure 4-7 Maxon RE 50 D.C. motor (PN 370354) Technical Data

4.3. Power and Torque Calculation

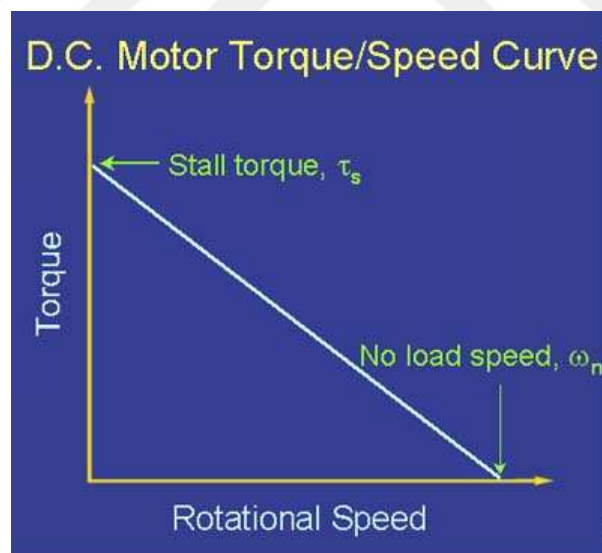


Figure 4-8 D.C. Motor Torque-Speed Curve

Figure 4.8 [23] above presents relation of torque and speed for a D.C. motor. As can be seen in the curve, torque and speed of the D.C. motor shaft are inversely proportional. The two important definitions to read a D.C. motor technical data sheet are the stall torque and no load speed. [23]

The torque is at its maximum at stall torque, T_s , however the *D.C.* motor shaft is not rotating. [23]

The *D.C.* motor shaft speed is at its maximum at no load speed, ω_n , (at that point, no torque applies to the motor shaft). [23]

In reality, a *D.C.* motor cannot be utilized across the entire torque-speed curve. An imaginary line separates the continuous range and the intermittent range. The limit established by this imaginary line is known as the maximum continuous torque and it approximately corresponds to 1/3 (one third) of the stall torque. In the continuous range, the *D.C.* motor can be used without any issues and time limitation, however the *D.C.* motor is may get overheated and damaged if it is exposed to this range for a long time. [24]

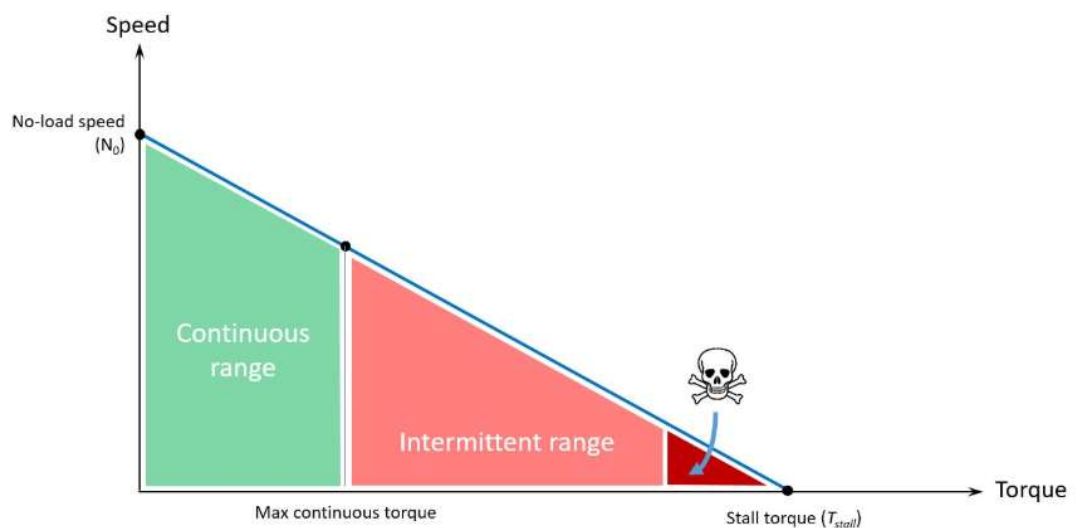


Figure 4-9 [24] *D.C.* Motor Speed – Torque Curve Showing Ranges

As shown in Figure 4.10 [23], the maximum power takes place at the point on which $T = 1/2 T_s$ and $\omega = 1/2 \omega_n$ based on the inversely linear relation of speed and torque. [23]

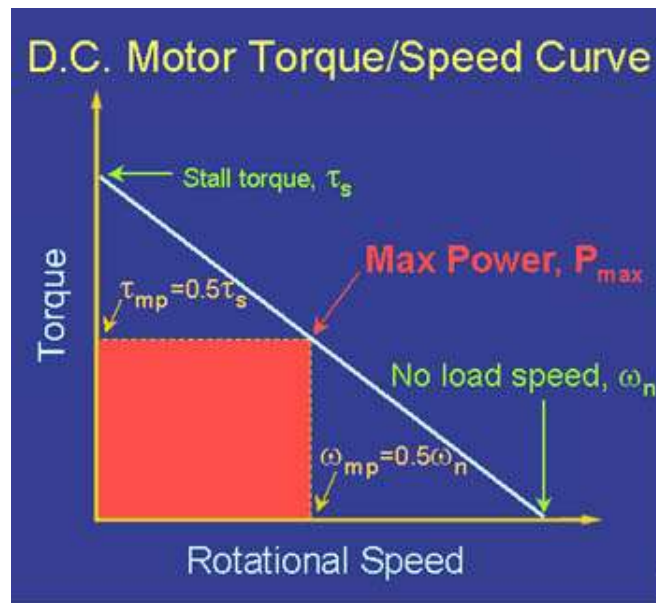


Figure 4-10 [23] D.C. Motor Torque Speed Curve

The inversely linear graph of the *D.C.* motor torque/speed is a very useful estimation. [23]

For that reason, torque - speed curve of the Maxon RE 50 *D.C.* motor (PN 370354) is generated and plotted as shown in Figure 4.11 below by the thesis author based on those *D.C.* Motor torque - speed fundamentals; and the technical specification (refer to Figure 4.7) of the *D.C.* motor provided by the manufacturer.

As for the finite element analysis (*FEA*), and therefore the topology optimization to be performed, we will be basing on the P_{max} condition of the *D.C.* motor in order to be more on the conservative side for the final design although we know that P_{max} condition falls into the intermittent range.

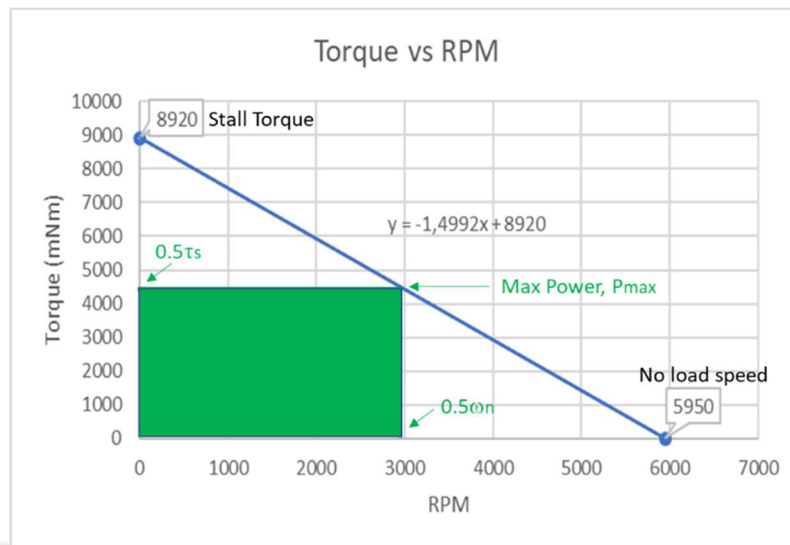


Figure 4-11 Torque - Speed Curve of Maxon RE 50 D.C. Motor

Power is defined as:

$$P = T \times \omega \quad (4.1)$$

where P represents power in watts, T represents torque in N.m and ω represents the rotational speed in rad/s. Therefore,

$$\text{Power (W)} = \text{Torque (N.m)} \times \omega \text{ (RPM)} / 9.549^*$$

$$P_{max} = [(8.920 \times 0.5) \times (5950 \times 0.5)] / 9.549 =$$

$$(4.46 \times 2975) / 9.549 = \underline{1390 \text{ W}} = \underline{1.39 \text{ kW}}$$

When P_{max} condition applies:

$$\underline{\text{Torque} = 4.46 \text{ Nm (4460 mNm)}} \text{ and } \underline{\text{RPM} = 2975}$$

*Note that 9.549 in above equation comes from

$$60 / 2\pi$$

4.4. Gear Force Analysis

As calculated above, 1.39 kW D.C. motor runs at 2975 RPM in clockwise direction as shown in Fig.4.12.

15 teeth helical pinions with 20° normal pressure angle, 1 mm normal module and a helix angle of 20° are keyed to the D.C. motor shafts.

We will be drawing a 3-dimensional sketch of the motor shaft and the pinion; and show the forces acting on the pinion.

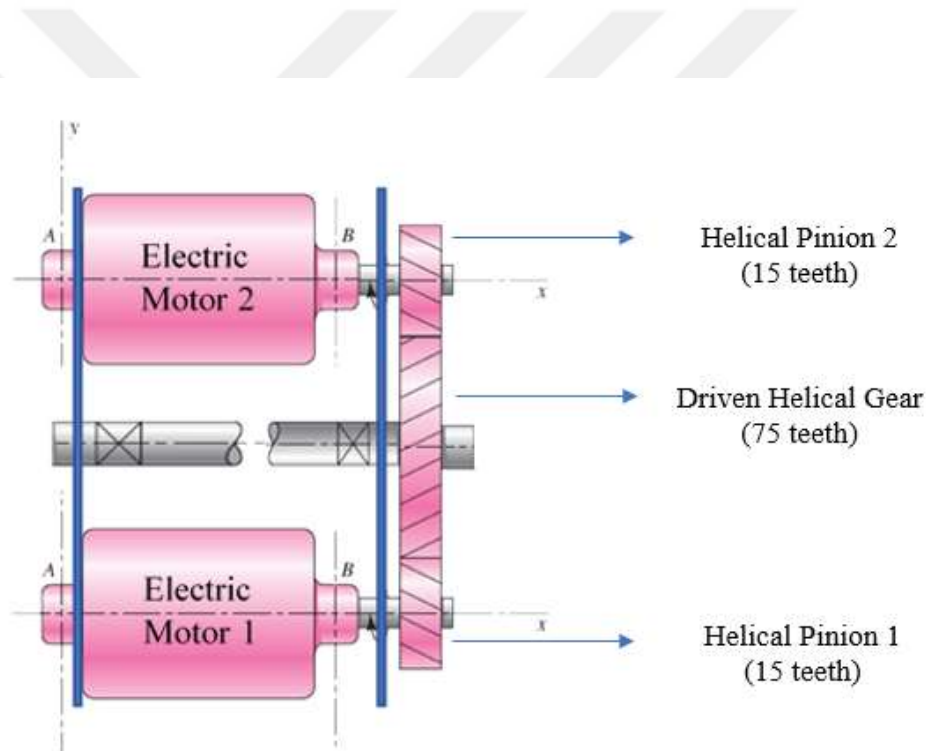


Figure 4-12 D.C. Motors and Gear Train

Given:

$$W=1.39 \text{ kW}$$

$$n_1=2975 \text{ RPM}$$

$$\Psi=20^\circ \text{ (helical angle)}$$

$$\Phi_n=20^\circ \text{ (normal pressure angle)}$$

$$m_n=1 \text{ mm (normal module)}$$

$$Z_1=15$$

$$Z_2=75$$

The transverse pressure angle for helical gear can be calculated with the use of below formula:

$$\tan \Phi_n = \tan \Phi \cos \Psi \quad (4.2)$$

Therefore, based on (4.2), the transverse pressure angle is:

$$\Phi = \tan^{-1} (\tan 20^\circ / \cos 20^\circ) = \tan^{-1} (0.38733^\circ) = \underline{21.17^\circ}$$

The module for a helical gear is defined as:

$$m = m_n / \cos \Psi \quad (4.3)$$

Based on (4.3), the module is:

$$m = 1 / \cos 20^\circ = \underline{1.0642 \text{ mm}}$$

The pitch diameter for helical gears is defined as:

$$d_1 = m Z_1 \quad (4.4)$$

Based on (4.4) the pitch diameter of the pinion is:

$$d_1 = 1.0642 \times 15 = 15.963 \text{ mm}$$

Pitch line velocity for a helical gear is defined as:

$$V = \pi d_1 n_1 / 60 \quad (4.5)$$

Based on (4.5), the pitch line velocity is:

$$V = \pi \times 15.963 \times 2975 / 60000 = 2.487 \text{ m/sec}$$

Acting forces are calculated as shown in below:

$$F_t = 1000 \text{ W} / V = 1000 \times 1.39 / 2.487 = 558.906 \text{ N}$$

$$F_r = F_t \tan \Phi = 558.906 \times \tan 21.17^\circ = 216.449 \text{ N}$$

$$F_a = F_t \tan \Psi = 558.906 \times \tan 20^\circ = 203.425 \text{ N}$$

$$F_n = F_t / \cos \Phi_n \cos \Psi = 558.906 / (\cos 20^\circ \times \cos 20^\circ) = 635.963 \text{ N}$$

The acting force F_r applies in the $-y$ direction, F_a applies in the x direction and F_t applies in the z direction at the pitch point C of the pinion as shown in Fig. 4.13.

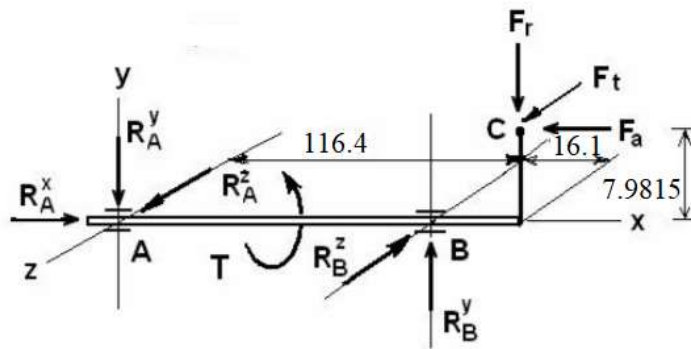


Figure 4-13 Free Body Diagram of Acting Forces at the Pitch Point C of the Pinion

For clarification purpose, Figure 4.14 shows the acting forces and their directions for Pinion-1 and the Driven Helical Gear. Likewise, Figure 4.15 shows the acting forces and their directions for Pinion-2 and the Driven Helical Gear.

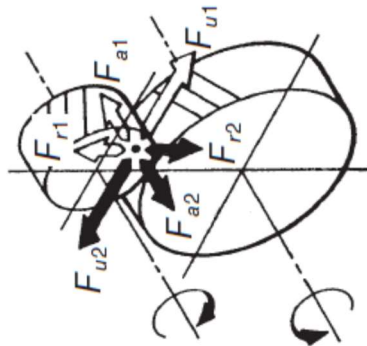


Figure 4-14 Pinion 1 and Driven Gear

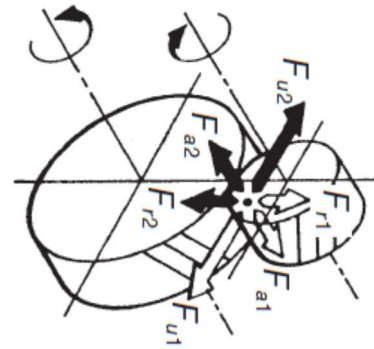


Figure 4-15 Pinion 2 and Driven Gear

Now, the *RPM* and torque of the driven gear shaft can both be calculated.

The gear ratio is defined as:

$$\text{Gear Ratio} = Z_2 / Z_1 \tag{4.6}$$

Therefore, the gear ratio is:

$$\text{Gear Ratio} = Z_2 / Z_1 = 75 / 15 = 5$$

So, at P_{max} , the rotational speed of the driven shaft will be:

$$n_1 \times Z_1 = n_2 \times Z_2$$

$$2975 \times 15 = n_2 \times 75$$

$$n_2 = 595 \text{ RPM}$$

$$\text{Gear Ratio} = Z_2 / Z_1 = \text{Torque out} / \text{Torque in}$$

$$5 = \text{Torque out} / \text{Torque in}$$

$$\text{Torque out} = 4.46 \times 5 = \underline{22.3 \text{ Nm} = 2230 \text{ mNm}}$$

5. DESIGN FOR ADDITIVE MANUFACTURING

In the present work, Altair Inspire™ 2019.1 was used as the software package for the topology optimization, *FEA* and redesign of EVRIM-4's Electric Motor Bracket.

Inspire™ is one of the industry leading Generative Design/Topology Optimization software products from Altair that is well known with its user friendly interface and capability of fast simulation solutions. It is a very useful and powerful tool for concept development that can provide savings and benefits in terms of engineering time, material utilization rate and therefore the weight of the component as well. [18]

Altair Inspire™ utilizes one of the most powerful structural optimization software OptiStruct™ as a solver in the background. [25]

The process map of the design steps followed in the present work is given in Figure 5.1 below.

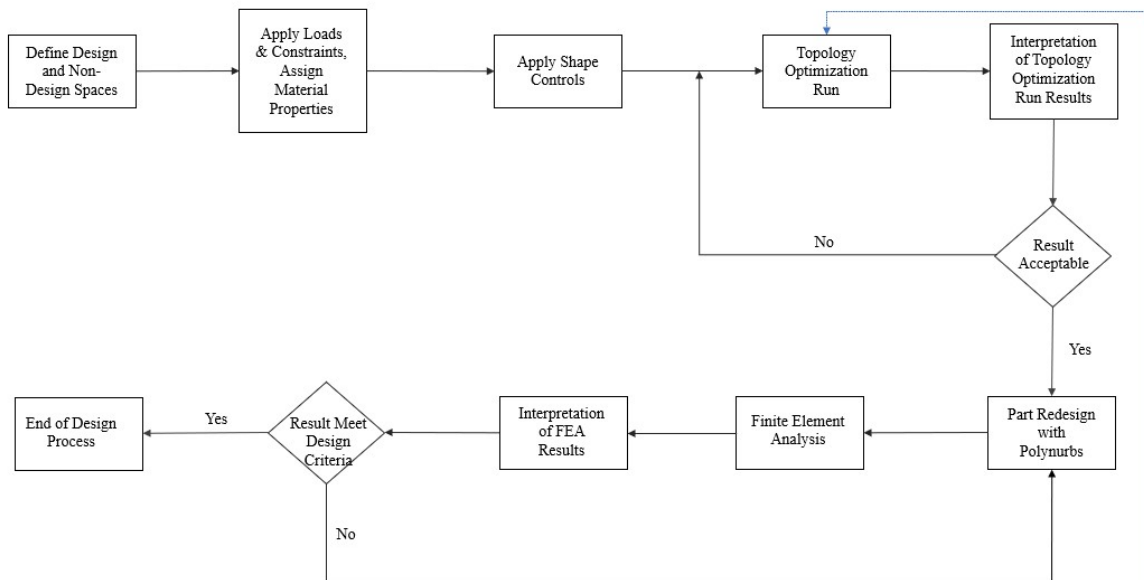


Figure 5-1 Process Map of Design Steps

5.1. Definition of Design and Non-Design Spaces

As the first step, design and non-design spaces need to be designated on the original design of the part. Design spaces indicates the portions of the part that will be altered mainly by material removal to generate the lightest structure which can resist the applied loads. In other words, design space is where density-based topology optimization will take place. Conversely, non-design spaces mean the portions of the part which cannot be modified such as fixation points, and therefore, will have to stay the same during and after the optimization. [20]

Generally, loads are not recommended to be applied to design spaces as it may lead to wrong and falsifying results. Rather than that, design and non-design spaces need to be designated and loads need to be applied to non-design spaces. [20]

By default, design spaces are shown in brown and non-design spaces are shown in Altair Inspire™ for a clear differentiation and representation. [20]

Figure 5.2 and Figure 5.3 show Design and Non-Design Spaces defined by the author on original model of the Electric Motor Bracket of EVRIM-4 Shell Eco-Marathon vehicle.

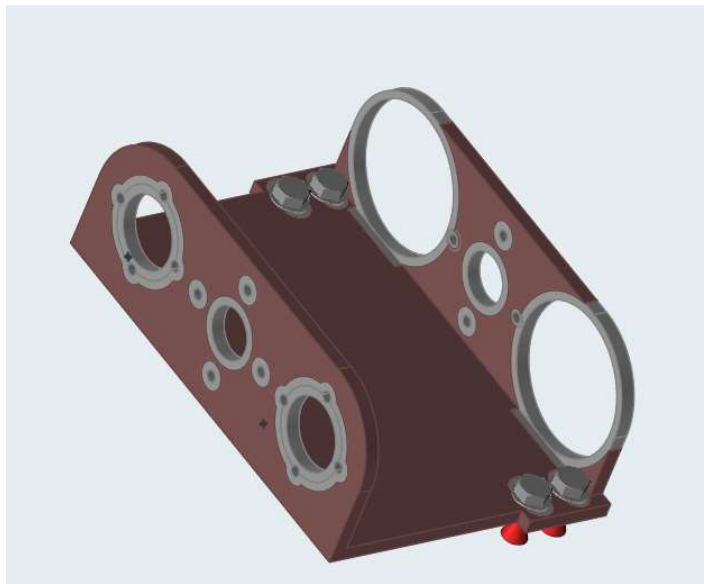


Figure 5-2 Design and Non-Design Spaces.

Gray areas show non-design spaces and brown areas show design spaces.

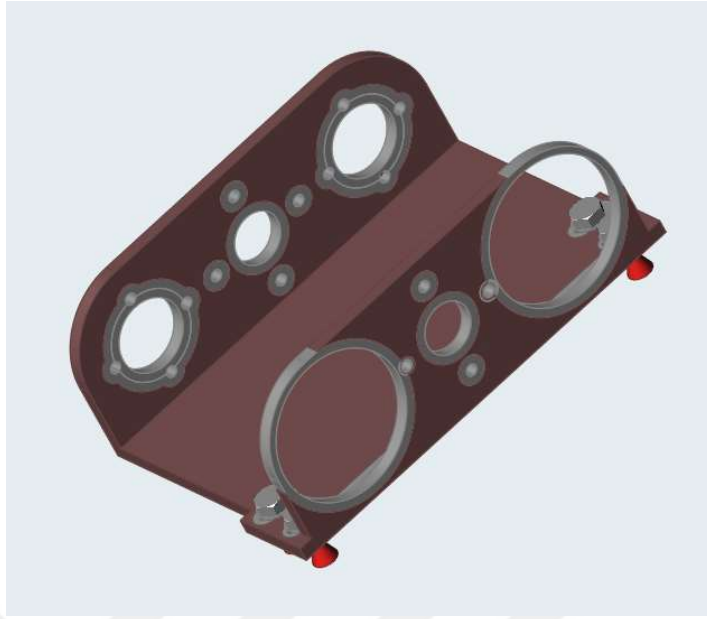


Figure 5-3 Design and Non-Design Spaces.

Gray areas show non-design spaces and brown areas show design spaces.

5.2. Definition of Loads, Constraints and Material Properties

Upon completion of definition of design and non-design spaces, the next step is to apply loads (forces, torque, masses, etc.) and constraints to the model of the original design. In the present work, loads described and calculated in Chapter 4 are applied to the non-design spaces of the model of the original Electric Motor Bracket design. The fixation points on the motor bracket are considered as the constraints. Figure 5.5 and Figure 5.6 represent multiple load cases and constraints applied to the model of the original design.

Material properties are also assigned / defined in this step. In the case of the original design of the Electric Motor Bracket, the part base material is *7075 Al* alloy. However, as *7075 Al* alloy is not a viable feedstock material option in today's additive manufacturing technologies / processes, *AlSi10Mg* which is commonly used as an alternate to *7075 Al* alloy is selected as the material option in this present work.

AlSi10Mg material technical data [26] [27] given in Figure 5.4 is entered into Altair Inspire™ material database for the accuracy of the analysis to be performed in the design process.

Material	E (GPa)	Poisson's Ratio	Density (g/cm³)	Yield Stress (MPa)	Tensile Strength (MPa)	CTE ($\mu\text{m/mK}$)
<i>AlSi10Mg</i>	70	0.33	2.67	215	335	20

Figure 5-4 Material data[26] [27] for *AlSi10Mg*

5.3. Applying Shape Controls

Without application of loads and constraints, it is not possible to perform topology optimization. That is not the case for the application of shape controls. Unlike loads and constraints, application of shape controls is optional. But, the aim of shape controls application is to ensure the design generated in Inspire™ is producible. For this reason, shape controls are used during the topology optimization phase, not during *FEA* phase. [28]

As also described above, shape controls relate to the manufacturing constraints. [20]

The two shape control types in Inspire™ are “symmetry” and “draw directions”. The use of both shape controls at the same time is not possible. Only one type can be selected. [29]

Out of the available draw direction tools in Inspire™, only “overhang” tool is compatible to additive manufacturing technology. The purpose of the “overhang” tool is to build self-supporting parts. Draw direction tools other than overhang tool are used for conventional processes, such as casting and extrusion. [29]

In this present work, overhang tool and symmetry tool are both used. Both Figure 5.4 and Figure 5.5 represent multiple load cases, constraints, overhang tool and symmetry tool applied to original design model.

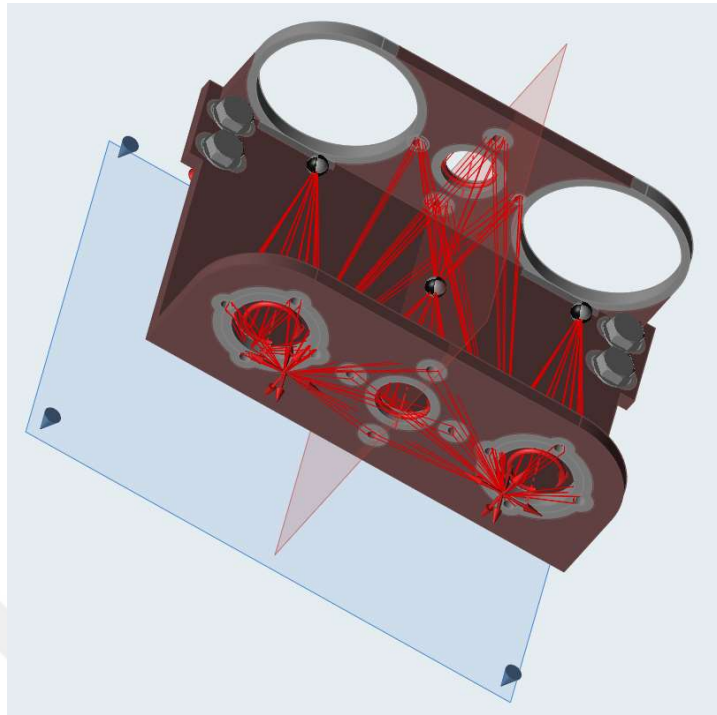


Figure 5-5 Multiple loads, constraints applied to original electric motor bracket model.
Overhang and symmetry shape control tools are also applied.

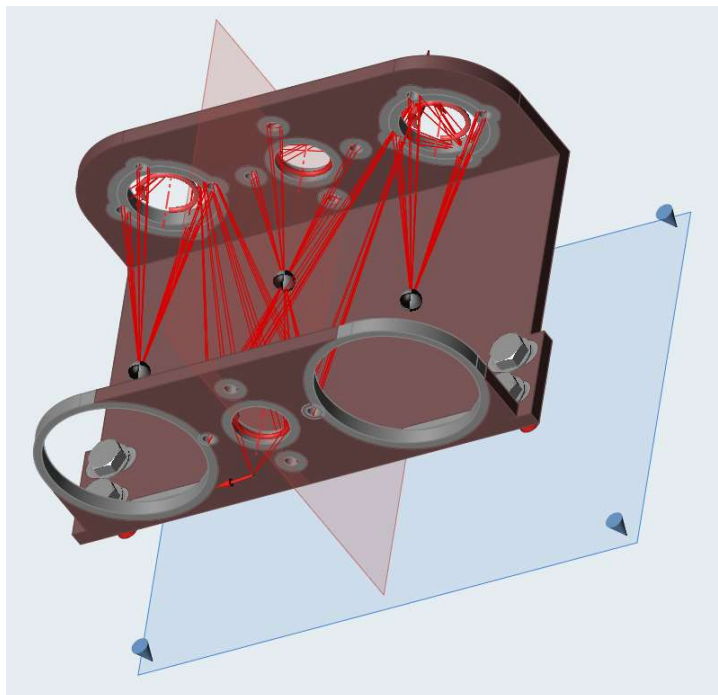


Figure 5-6 A different view of multiple loads, constraints applied to original electric motor bracket model.
Overhang and symmetry shape control tools are also applied.

5.4. Topology Optimization Run

After definition of loads, constraints, material properties and application of shape controls, the next step is to perform the topology optimization run.

In topology optimization applications, the material removal takes place within the portions defined as design spaces, aiming to generate the lightest structure that is capable of resisting applied loads. In this method, while attempting to get the lightest structure, it is recommended to maximize the stiffness of the part as much as it is possible. [30] In a topology optimization run, Altair Inspire™ offers designers to select Maximize Stiffness or Minimize Mass as the objective of the run.

If the design engineer chooses stiffness maximization as the objective of the topology optimization run, the consequential structure will withstand deflection. On the contrary, if the designer selects mass minimization as the objective, the consequential structure becomes lighter. The amount of deflection will be higher in the case of mass minimization in comparison to stiffness maximization. [30] For this reason, stiffness maximization is selected by the author in this present work as the objective of the topology optimization run in order to ensure durability of the redesigned part.

After selection of objective of the topology optimization run, the design engineer needs to choose the constraints. If stiffness maximization is chosen as the objective of the run, a mass target needs to be defined for the optimization and this target needs to be entered to Inspire™. [31]

In Inspire™, the wall thickness of the structure can also be determined by the designer. If the designer chooses a very small thickness as the constraint, the cycle time of the optimization gets longer. The software package is capable of determining the minimum thickness taking average size of elements in the model into account. [32]

In order to keep the optimization time reasonable, the author has selected the default values in Inspire™ software while performing the present work. Figure 5.7 and Figure 5.8 show the part in optimized condition from different views.



Figure 5-7 Part After Topology Optimization Run

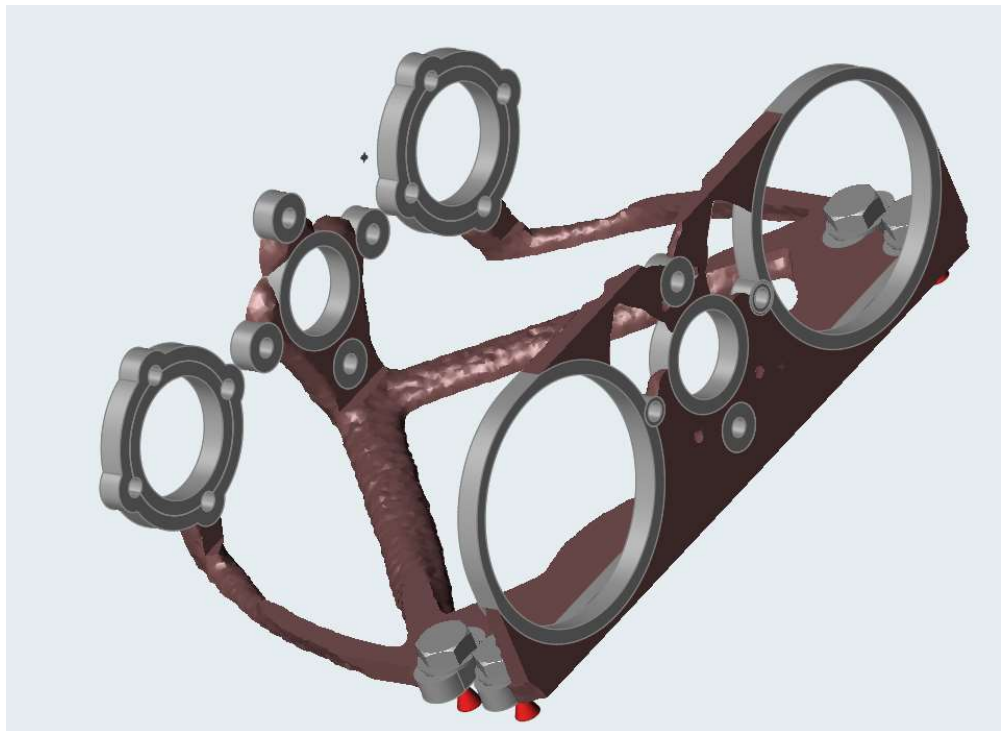


Figure 5-8 Another View of the Part After Topology Optimization Run

5.5. Interpretation of Topology Optimization Results

Once the optimization run is complete, the material distribution in the optimized geometry has been checked and believed to be a promising result to proceed with the next steps of the design process.

An important thing in this phase is to perform a *FEA* to verify if the optimized part will be safe enough to withstand the loads to which it will be exposed to while in operation. Because, if there are any major issues with safety of the part in this phase, there is no need to move to the next phase. For this reason, von Mises stress analysis was performed on the optimized model upon completion of the optimization run. Figure 5.9 show the von Mises stress analysis results of the optimized model.

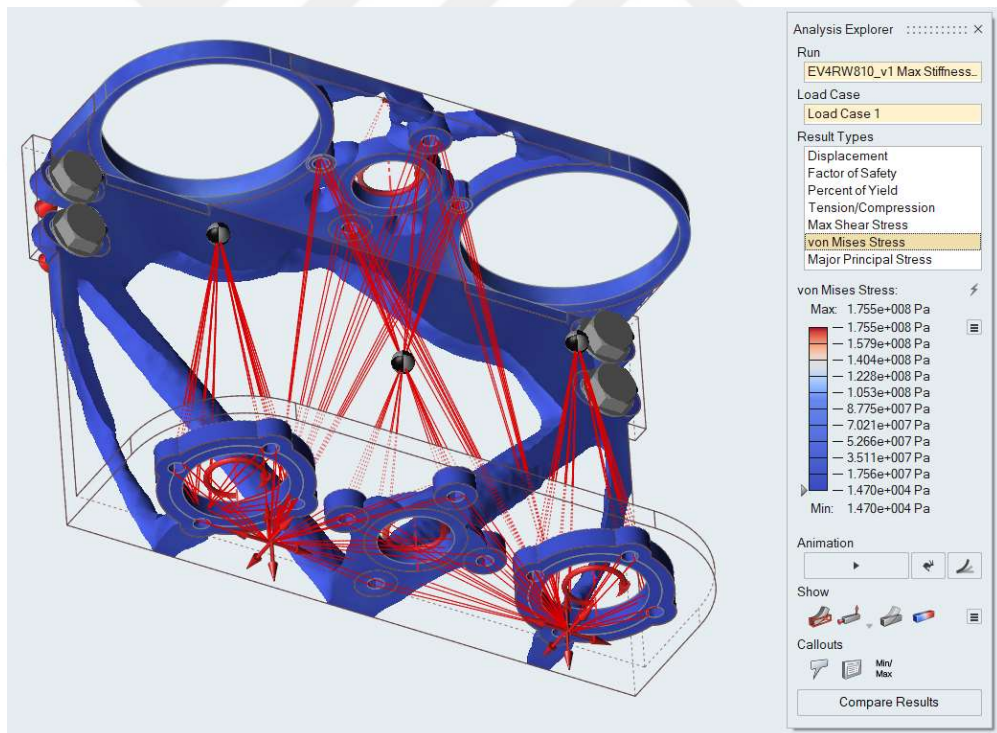


Figure 5-9 von Mises Stress Analysis Results of the Optimized Model

As also shown in the von Mises Stress results slider of Figure 5.9, the maximum stress is found to be $1.755 \times 10^8 \text{ Pa}$ as the result of the von Mises stress analysis. The yield stress of *AlSi10Mg* material is $2.15 \times 10^8 \text{ Pa}$ (refer to Figure 5.4); therefore, the analysis supports

the fact that the optimized model will be well within the elastic zone even the *D.C.* Electric Motors are operating at P_{max} condition. Depending on this analysis result, the optimized model is found to be safe enough to move forward with the Part Design phase.

5.6. Setting Design Criteria

In order to verify reliability and structural capability of a component, the factor of safety is calculated. Choosing appropriate factor of safety is of critical importance in design process and it is based on various parameters. [33]

It does not mean the reliability and structural capability is assured with a high safety factor. [34]

For instance, the minimum required ultimate *FoS* in the present aviation business is 1.5. It is also known that that an ultimate *FoS* of 1.4 has been utilized in different spaceships up to now. [34]

In the selection of appropriate factor of safety, material properties are the key criteria. In general, lower factor of safety values are selected for ductile materials (majority of metals). On the other hand, higher factor of safety values are selected for brittle materials. [33]

Materials' plastic deformation ability without fracture under tensile loading is called ductility. As aluminum is known to be the sixth most ductile metallic material, *AlSi10Mg* material which is classified as an aluminum alloy is also considered to be a ductile metallic material. Basing on this, Tsirogiannis [33] defined the yielding safety factor for the *AlSi10Mg* alloy as 1.25 in his study. [33]

In this present work, a safety factor of 1.25 will be used for yield strength in this thesis as well. In addition, von Misses stress analysis will be performed to verify if the final design will still be in the elastic zone when the *D.C.* electric motors are operating at P_{max} condition.

5.7. Part Redesign with Inspire PolyNURBS

PolyNURBS is a modern modeling tool with which free-form smooth geometries can be generated from the optimized structures. Beyond being an easy to use toolset, it also enables faster solutions with a high accuracy. [35]

Another advantage that PolyNURBS tool brings is that the output results from the PolyNURBS tool can directly be utilized to produce final product via Additive Manufacturing. [35][20]

The model redesigned with the use of PolyNURBS tool is represented in Figure 5.10 and Figure 5.11.



Figure 5-10 Redesigned Model with the Use of PolyNURBS



Figure 5-11 Another view of Redesigned Model with the use of PolyNURBS

5.8. Rendering with Evolve

Evolve™ is a software package from Altair which offers rendering and hybrid modeling. [36]

It is a premium rendering software which can be utilized as a complementary tool to process Inspire™ results.

In this present work, upon completion of part design with the use of PolyNURBS tool in Altair Inspire™, Altair Evolve™ software has been used for rendering purpose in order to get photo-realistic images of the redesigned electric motor bracket. Figure 5.12 through Figure 5.14 shows the realistic images of the redesigned electric motor bracket after rendering the polyNURBS model with Altair's Evolve™ software.



Figure 5-12 Realistic Image of Redesigned Model After Rendering in Evolve Software



Figure 5-13 Another Realistic Image of Redesigned Model After Rendering in Evolve Software

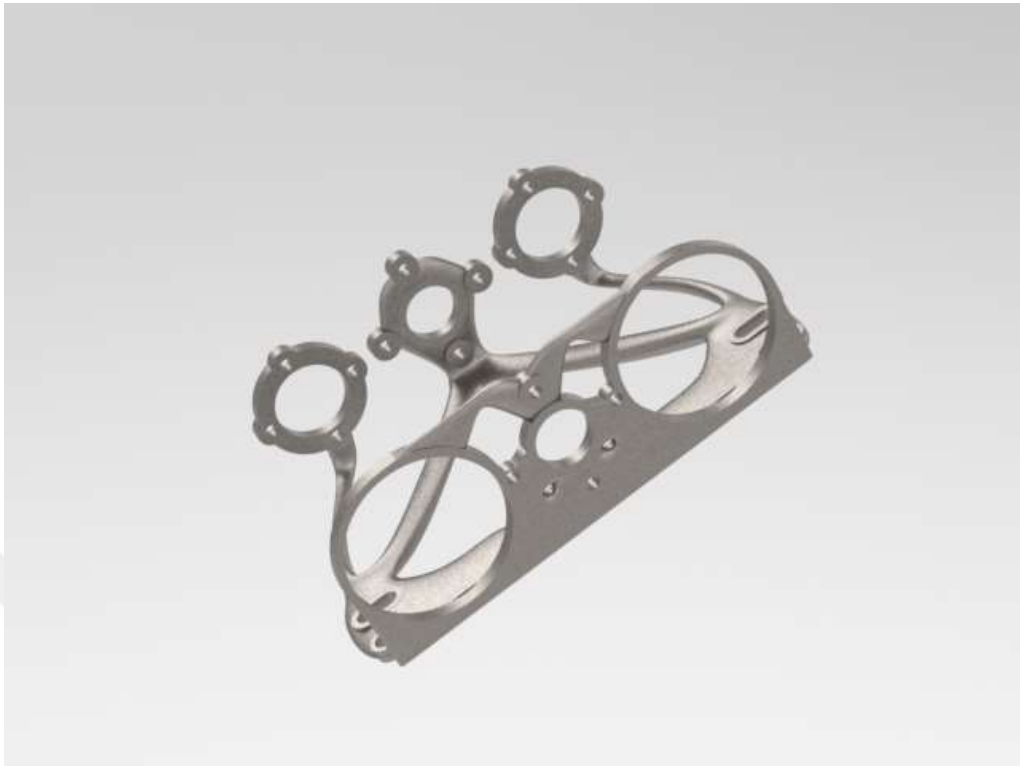


Figure 5-14 Another Realistic Image of Redesigned Model After Rendering in Evolve Software

6. RESULTS AND DISCUSSION

6.1. Mass of the Redesigned Model

A mass comparison was made between the original model and the redesigned model of the electric motor bracket. The calculated mass of the redesigned part is 229 grams per Altair Inspire™ analysis. Considering the mass of the original part design is 364 grams, redesign of electric motor bracket for additive manufacturing via Altair Inspire on the basis of topology optimization has reduced the mass of the part 37% (135 grams).

6.2. Waste Minimization with the Redesigned Model

Another important advantage of the redesigned model and its production with the use of additive manufacturing over the original design and original manufacturing technique will be relevant to waste minimization. As also highlighted in Section 4.2, it is calculated that 2837 grams of 7075 Al alloy billet would be needed to produce the original electric motor bracket via the original conventional subtractive techniques. Considering that the mass of the original design is 364 grams, 87% (2473 grams) of the material may be wasted to produce the electric motor bracket in the original method.

However, in the case of the redesigned model and its realization with the proposed *AM* technique brings the advantage of eliminating 2473 grams of material wasted in original subtractive method. Also, per Section 6.1, considering the mass reduction was in the redesigned part was 135 grams, adding the eliminated waste of 2473 grams on top of it, with the redesigned model and proposed *AM* technology, 2608 grams of material will be saved in comparison to the original design and subtractive manufacturing of the electric motor bracket.

6.3. Finite Element Analysis of PolyNURBS Results

A finite element analysis was performed with Altair Inspire™ to verify the ability of the redesigned model to withstand the loads it would be exposed to without any performance issues. In this aspect, factor of safety for yielding, ultimate factor of safety and von Mises stress analyses were performed.

The results of the analysis for factor of safety for yielding are given in Figure 6.1 through Figure 6.3.

The results of ultimate factor of safety are given in Figure 6.4 through Figure 6.6 and von Mises stress analysis results are given in Figure 6.7 and Figure 6.8.

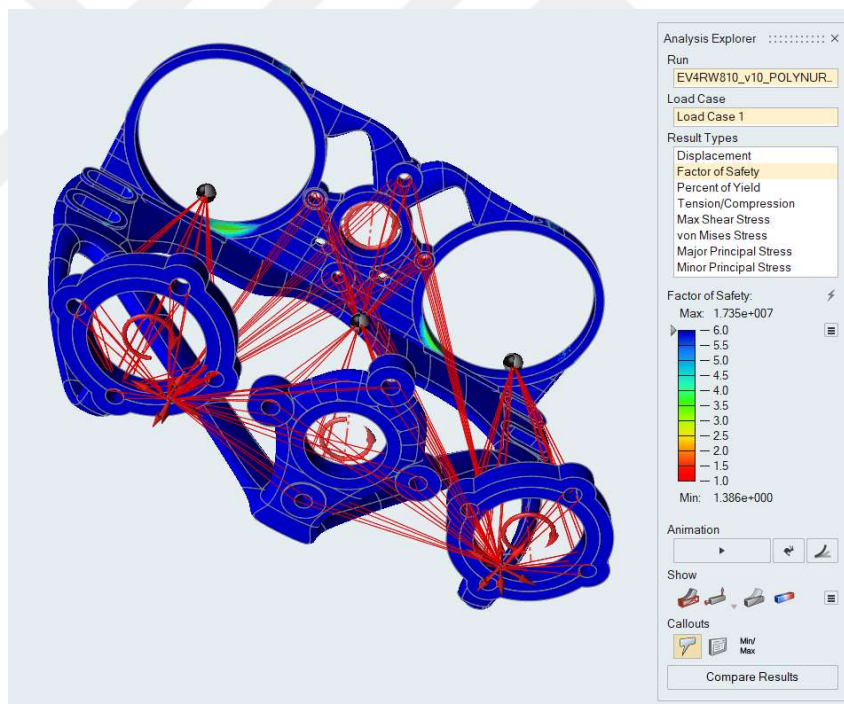


Figure 6-1 Analysis Results for Factor of Safety for Yielding.

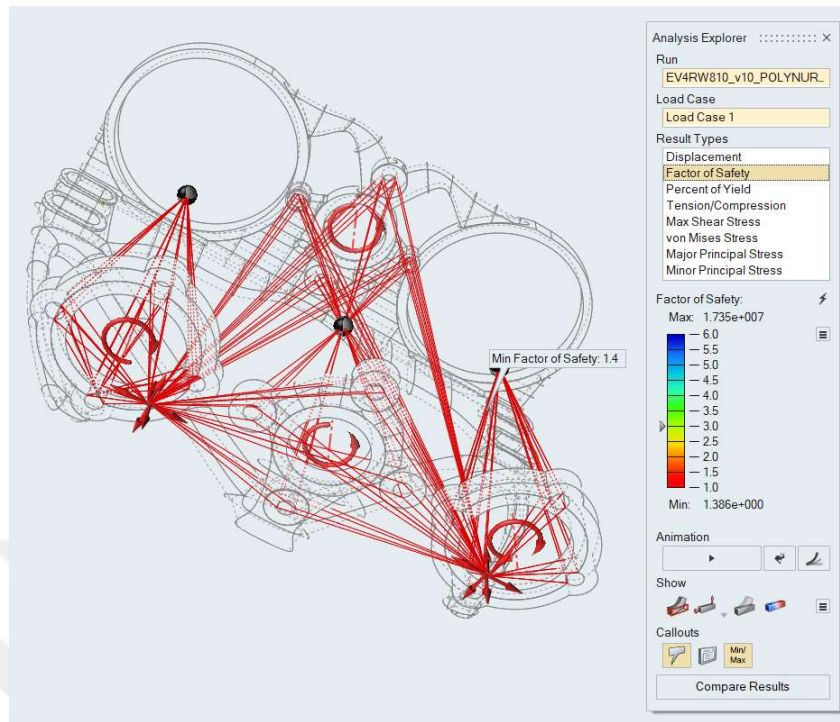


Figure 6-2 Analysis Results for FoS for Yielding Showing Minimum FoS Location.

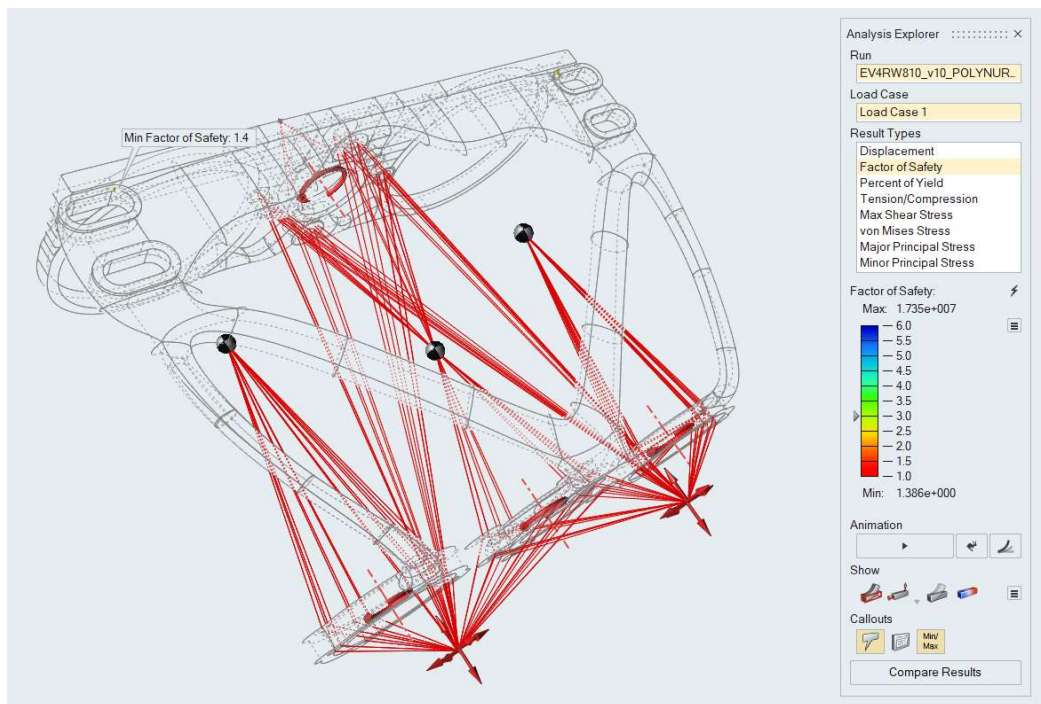


Figure 6-3 Analysis Results for FoS for Yielding Showing Minimum FoS Location.

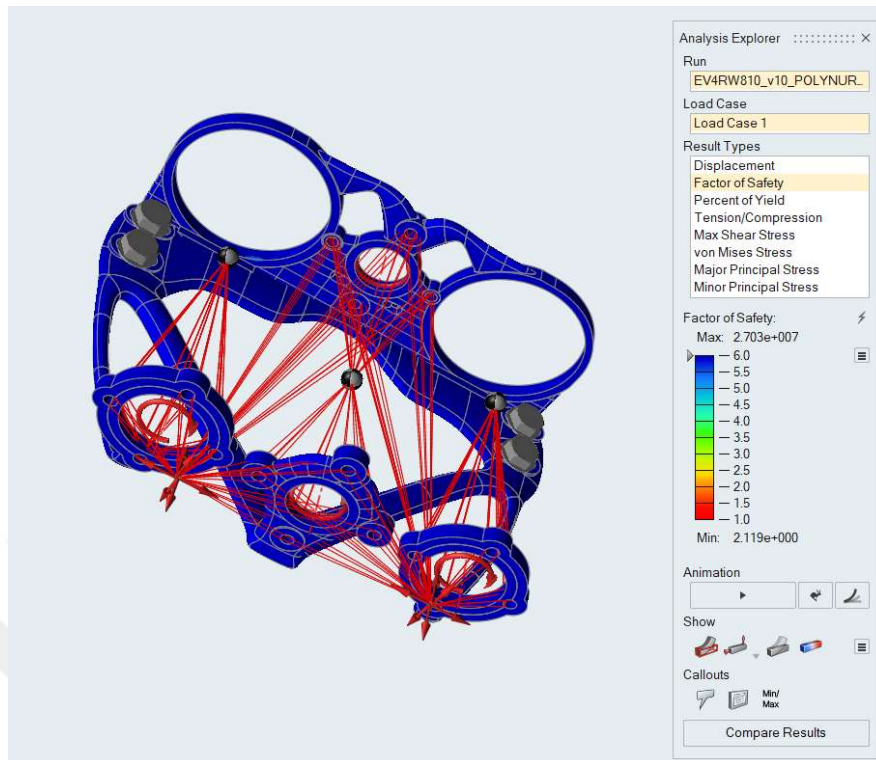


Figure 6-4 Analysis Results for Ultimate Factor of Safety

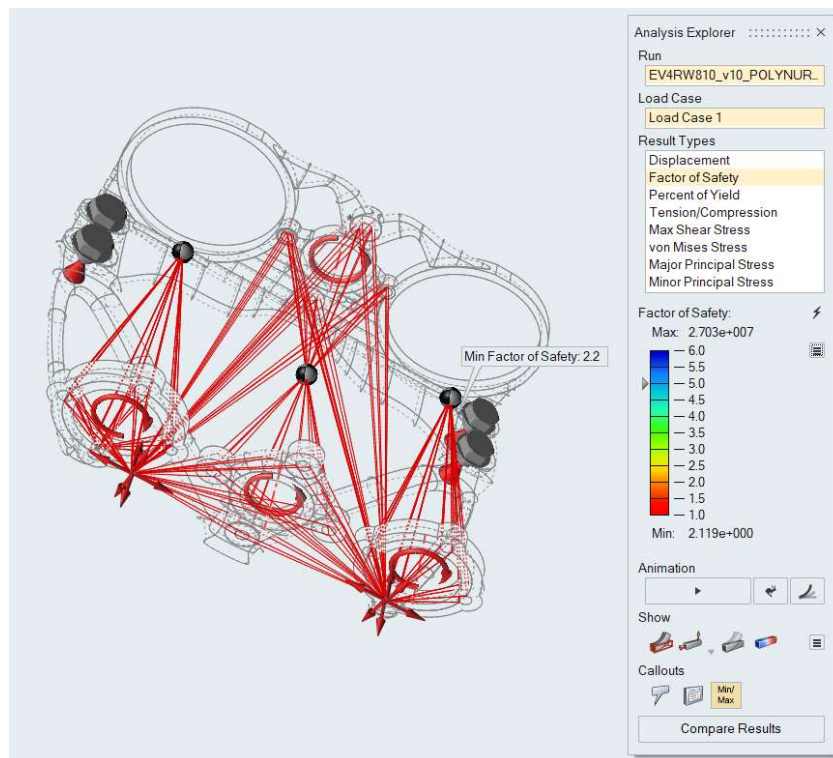


Figure 6-5 Analysis Results for Ultimate *FoS* showing Minimum Ultimate *FoS* Location.



Figure 6-6 Analysis Results for Ultimate *FoS* showing Minimum Ultimate *FoS* Location

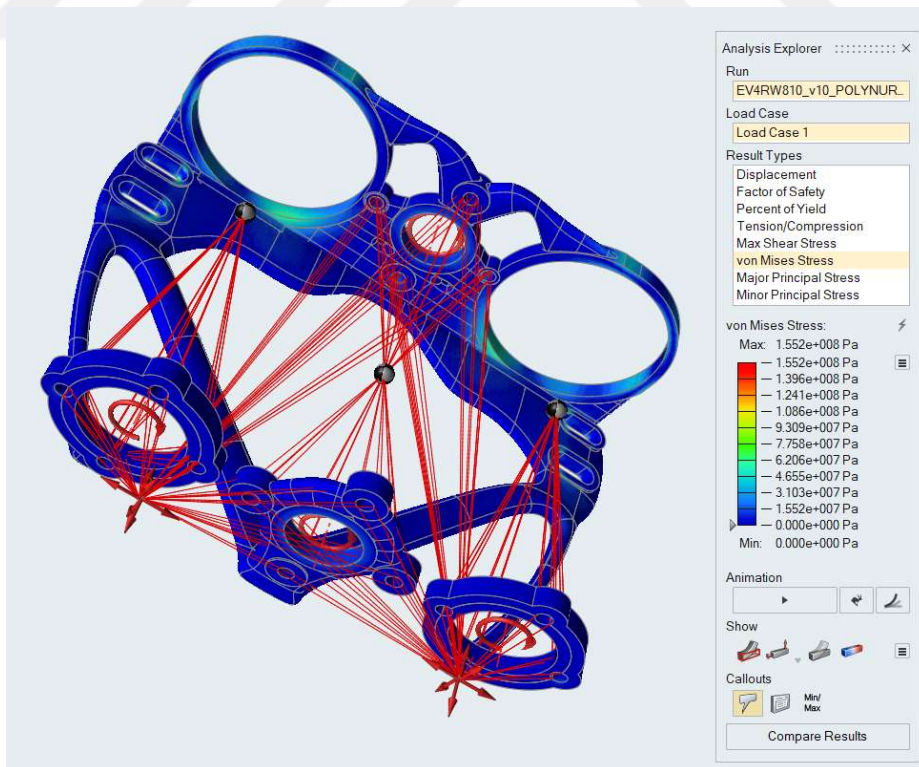


Figure 6-7 Analysis Results for von Misses Stress

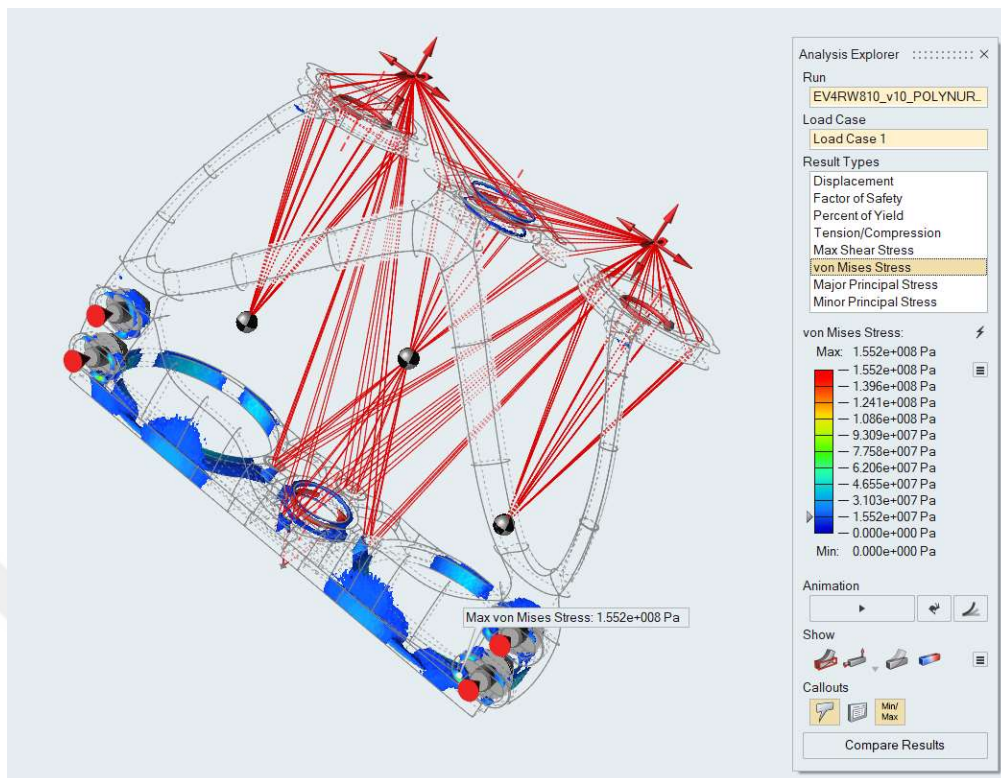


Figure 6-8 von Misses Stress Analysis Results Showing Maximum Stress Location.

6.4. Interpretation of Finite Element Analysis Results

As can be seen in results slider of Figure 6.1 through Figure 6.3, the minimum factor of safety for yielding is 1.4 and is above the design criteria of 1.25. This result makes it clear that the maximum load that applies to the electric motor bracket during operation will not move the component to outside of elastic zone in its stress - strain curve as intended.

Particular location of the minimum factor of safety for yielding is shown in Figure 6.2 and Figure 6.3 for information purpose.

An additional analysis for the ultimate factor of safety was performed and it is found to be ~2.1 as shown in Figure 6.4 through Figure 6.6. The calculated ultimate factor of safety of ~2.1 also exceeds the aforementioned (refer to Section 5.4) common aerospace standard of 1.5.

Finally, von Mises stress analysis was performed and the results from this analysis in Figure 6.7 and Figure 6.8 clearly show that the maximum stress is found to be $1.552 \times 10^8 \text{ Pa}$. As indicated earlier in Figure 5.4, the yield stress of *AlSi10Mg* material is $2.15 \times 10^8 \text{ Pa}$, and therefore the part will be well within the elastic zone even at P_{max} condition - to which the drivetrain will never be continuously exposed, see Section 4.3 in this thesis report – according to the von Mises stress analysis as well.

Based on all these analyses performed on the redesigned model, the design criteria has been met; and it is verified that the part will be functioning within the elastic behavior zone in its stress-strain curve even at maximum loading condition.



7. CONCLUSIONS AND RECOMMENDATIONS

Additive manufacturing is an emerging technology and its popularity has increased a lot in the last few years. Companies, including but not limited to aerospace and automotive industries would like to implement the additive manufacturing technology on more components to benefit from the offerings of the technology such as design freedom, lightweight structures, waste minimization and so on.

In the present work, the original model of the electric motor bracket made of 7075 Al alloy has been redesigned successfully with the use Altair Inspire™ software on the basis of topology optimization methodology for its production with the use of additive manufacturing.

The redesigned part is proposed to be manufactured with the use of *AlSi10Mg* alloy which is the most common Al alloy for additive manufacturing applications. Per the finite element analysis of the redesigned structure considering the loads that it will be subjected to at P_{max} condition of the *D.C.* motors, it has a minimum safety factor of 1.4 for yielding which has met the design criteria of 1.25.

In addition, the mass of the redesigned part is reduced by 37%, from 364 grams to 229 grams and 87% waste reduction will be achieved in comparison to the original design and original manufacturing method.

As can also be seen from the present work, the redesigned model for its realization via additive manufacturing brings significant advantages in terms of mass reduction and waste minimization while it still meets the design criteria and is expected to function without any structural failure.

It is recommended to proceed with the additive manufacturing process of the redesigned model, during which part processing parameters may need to be developed and established. During that phase, if needed, modifications in the new part design may be considered to support producibility.

REFERENCES

- [1] ASTM INTERNATIONAL, “ASTM F2792-12a,” *Rapid Manuf. Assoc.*, pp. 1–3, 2013.
- [2] I. Gibson, D. Rosen, and B. Stucker, “Additive manufacturing technologies: 3D printing, rapid prototyping, and direct digital manufacturing, second edition,” *Addit. Manuf. Technol. 3D Printing, Rapid Prototyping, Direct Digit. Manuf. Second Ed.*, no. 3, pp. 1–498, 2015.
- [3] “(No Title).” [Online]. Available: https://cdn0.scrvt.com/eos/205d38720e3a566b/64319de7c39a/EOS_Whitepaper_GoAdditiveAndBeDisruptive_en_WEB.pdf. [Accessed: 25-Dec-2019].
- [4] K. Soderhjelm, “Topology Optimization for Additive Manufacturing,” 2017.
- [5] A. Clausen, *Topology Optimization for Additive Manufacturing*, vol. 1, no. September. 2015.
- [6] “Shell Eco-marathon | Shell Global.” [Online]. Available: <https://www.shell.com/make-the-future/shell-ecomarathon.html>. [Accessed: 12-Nov-2019].
- [7] “ADDITIVE MANUFACTURING FEASIBILITY STUDY & TECHNOLOGY DEMONSTRATION EDA AM State of the Art & Strategic Report.”
- [8] P. EDLUND, “Additive Manufacturing in Low-volume Production Business Case for Metal Components,” p. 60, 2017.
- [9] T. Gornet, “History of Additive Manufacturing,” pp. 1–24, 2017.
- [10] A. M. Driessen, “Overhang constraint in topology optimization for additive manufacturing: a density gradient based approach,” pp. 1–85, 2016.
- [11] O. Diegel, A. Nordin, and D. Motte, *A Practical Guide to Design for Additive Manufacturing*. 2019.
- [12] A. Verbart, *Topology Optimization with Stress Constraints*. 2015.
- [13] J. Liu *et al.*, “Current and future trends in topology optimization for additive manufacturing,” *Struct. Multidiscip. Optim.*, vol. 57, no. 6, pp. 2457–2483, 2018.
- [14] M. Langelaar, “An additive manufacturing filter for topology optimization of print-ready designs,” *Struct. Multidiscip. Optim.*, vol. 55, no. 3, pp. 871–883, 2017.
- [15] S. Johnsen, “Structural Topology Optimization: Basic Theory, Methods and Applications,” 197, 2013.
- [16] E. Atzeni and A. Salmi, “Economics of additive manufacturing for end-usable metal parts,” *Int. J. Adv. Manuf. Technol.*, vol. 62, no. 9–12, pp. 1147–1155, 2012.
- [17] J. Plocher and A. Panesar, “Review on design and structural optimisation in additive manufacturing: Towards next-generation lightweight structures,” *Mater. Des.*, vol. 183, p. 108164, 2019.

- [18] “Altair Inspire: Generate Structurally Efficient Concepts Quickly and Easily.” [Online]. Available: <https://solidthinking.com/product/inspire/>. [Accessed: 19-Nov-2019].
- [19] “(No Title).” [Online]. Available: <https://enginsoftusa.com/pdfs/Altair-SolidThinking-Products.pdf>. [Accessed: 23-Nov-2019].
- [20] [https://cdn2.hubspot.net/hubfs/47251/altairuniversity-ebooks\(Matthias\)/Simulation_Driven_Design_with_Inspire_eBook.pdf](https://cdn2.hubspot.net/hubfs/47251/altairuniversity-ebooks(Matthias)/Simulation_Driven_Design_with_Inspire_eBook.pdf).
- [21] “maxon - Online Shop.” [Online]. Available: <https://www.maxongroup.com/maxon/view/product/370354>. [Accessed: 16-Nov-2019].
- [22] “(No Title).” [Online]. Available: http://www.ensatek.com.tr/image/urun/re/36RE50_200.pdf. [Accessed: 16-Nov-2019].
- [23] “D.C. Motor Torque/Speed Curve Tutorial::Understanding Motor Characteristics.” [Online]. Available: <http://lancet.mit.edu/motors/motors3.html>. [Accessed: 16-Nov-2019].
- [24] “Get to know your DC motor: how to read a datasheet - luosrobotics - Medium.” [Online]. Available: <https://medium.com/luosrobotics/how-to-read-a-dc-motors-datasheet-f70fa440452b>. [Accessed: 16-Nov-2019].
- [25] “Top 5 things You Need to Know About the Altair Inspire™ Platform - The Altair Blog.” [Online]. Available: <https://blog.altair.com/top-5-things-you-need-to-know-about-the-altair-inspire-platform/>. [Accessed: 24-Nov-2019].
- [26] “(No Title).” [Online]. Available: https://gpiprototype.com/pdf/EOS_Aluminium_AlSi10Mg_en.pdf. [Accessed: 23-Nov-2019].
- [27] “Aluminum 360.0-F Die Casting Alloy.” [Online]. Available: <http://www.matweb.com/search/datasheet.aspx?matguid=46cc3a20683748718693cb6039bec68&ckck=1>. [Accessed: 23-Nov-2019].
- [28] “Inspire 2015 - Shape Controls.” [Online]. Available: https://solidthinking.com/training/2015/inspire/content/opti_setup/shape_controls.htm. [Accessed: 23-Nov-2019].
- [29] “Altair Inspire: Generate Structurally Efficient Concepts Quickly and Easily.” [Online]. Available: [https://solidthinking.com/support-training/inspire/?keywords=shape controls](https://solidthinking.com/support-training/inspire/?keywords=shape%20controls). [Accessed: 23-Nov-2019].
- [30] “Structure > Run > Optimization > Topology Optimization.” [Online]. Available: https://solidthinking.com/help/Inspire/2017/win/en_us/topology_optimization.htm. [Accessed: 24-Nov-2019].
- [31] “Structure > Run > Optimize > Run Optimization > Mass Targets.” [Online]. Available: https://solidthinking.com/help/Inspire/2016/win/en/mass_targets.htm. [Accessed: 24-Nov-2019].
- [32] “Structure > Run > Optimization > Optimization Constraints > Thickness

- Constraints.” [Online]. Available:
https://solidthinking.com/help/Inspire/2018/win/en_us/thickness_controls.htm.
[Accessed: 24-Nov-2019].
- [33] E. C. Tsirogiannis, *Reverse Engineering , Redesign and Topology Optimization for Additive Manufacturing of an Industrial Robot Arm Link National Technical University of Athens Interdisciplinary Postgraduate Programme on Automation Systems Direction : Manufacturing and Produ*, no. January. 2019.
- [34] J. J. Zipay, C. T. Modlin, and C. E. Larsen, “The ultimate factor of safety for aircraft and spacecraft – its history, applications and misconceptions,” *57th AIAA/ASCE/AHS/ASC Struct. Struct. Dyn. Mater. Conf.*, 2016.
- [35] “Inspire 2018 - Why Use PolyNURBS?” [Online]. Available:
https://solidthinking.com/training/2018/inspire/content/polynurbs/why_polynurbs.htm. [Accessed: 24-Nov-2019].
- [36] “Evolve: 3D Product Design and Rendering Software.” [Online]. Available:
<https://solidthinking.com/product/evolve/>. [Accessed: 26-Nov-2019].

CURRICULUM VITAE

AHMET ERKAN KILIC

CONTACT DETAILS

Address : Orhan M. Gaffar Okkan Sk. No: 12/12, 41100, Izmit - Turkey

Email : aerkankilic@gmail.com

Cell : +90-532-392 5865

EDUCATION

09/2017- Present Piri Reis University
Graduate School of Science and Engineering
Master of Science in Mechanical Engineering (Solid Mechanics)

02/2008- 8/2010 Yeditepe University , Istanbul - Turkey
The Institute of Social Sciences
Masters in Business Administration (MBA)

09/1998-06/2003 Sakarya University, Sakarya - Turkey
Faculty of Engineering
Department of Metallurgical and Materials Engineering

09/1991-09/1998 Sekine Evren Anatolian High School, Manisa - Turkey
Science-Maths

FOREIGN LANGUAGES

Good command of both written and spoken English.

WORK EXPERIENCE

- 9/2015- Present* GE Aviation, Gebze-Turkey
Coating Primary Laboratory Leader
Senior Engineer, Coatings
- 7/2014- 9/2015* GE Aviation, Gebze-Turkey
Engineering Manager
Coatings & Chemical Processes
- 11/2008 - 7/2014* GE Aviation, Gebze-Turkey
Team Leader
Coatings, Chemical Processes and Joining Technologies
- 09/2005 – 11/2008* GE Aviation, Gebze-Turkey
Lead Engineer
Coating & Chemical Processes
- 07/2004-09/2005* DekorPan Isı Sistemleri Ltd.Sti, İzmir-Turkey
Process Engineer
Electroplating Plant

CLUB/ASSOCIATION MEMBERSHIP

- Member of SAWE (Society of Allied Weight Engineers)
- Member of ASM Thermal Spray Society